

Order Parameter Symmetries in High Temperature Superconductors

R. A. Klemm,¹ C. T. Rieck² and K. Scharnberg²

¹Materials Science Division, Argonne National Laboratory, Argonne, IL 60439 USA

²Fachbereich Physik, Universität Hamburg, Jungiusstraße 11, D-20355 Hamburg, Germany

(June 18, 2018)

The symmetry operations of the crystal groups relevant for the high temperature superconductors HgBa₂CuO_{4+δ} (Hg1201), YBa₂Cu₃O_{7-δ} (YBCO), and Bi₂Sr₂CaCu₂O_{8+δ} (BSCCO) are elucidated. The allowable combinations of the superconducting order parameter (OP) components are presented for both the angular momentum and lattice representations. For tetragonal Hg1201, the spin singlet OP components are composed from four sets of compatible basis functions, which combine to give the generalized *s*-, $d_{x^2-y^2}$ -, d_{xy} -, and $g_{xy(x^2-y^2)}$ -wave OPs. Although YBCO and BSCCO are both orthorhombic, they allow different mixing of these components. In YBCO, the elements of those *s*- and $d_{x^2-y^2}$ -wave sets (and of those d_{xy} - and $g_{xy(x^2-y^2)}$ -wave sets) are compatible, but in BSCCO, elements of *s*- and d_{xy} - wave sets (and of $d_{x^2-y^2}$ - and $g_{xy(x^2-y^2)}$ -wave sets) are compatible. The Josephson critical current density J_c^J across *c*-axis twist junctions in the vicinity of T_c is then evaluated as a function of the twist angle ϕ_0 , for each allowable OP combination, for both coherent and incoherent tunneling. For tight-binding Fermi surfaces, we argue that coherent tunneling is only possible for $\phi_0 = 0^\circ, 90^\circ$, for which the rotated Fermi surfaces line up. Recent experiments of Li *et al.* demonstrated the independence of $J_c^J(\phi_0)/J_c^S$ upon ϕ_0 at and below T_c , where J_c^S is the critical current density of a constituent single crystal. These experiments are shown to be consistent with an OP containing an *s*-wave component, but *inconsistent* with an OP containing the purported $d_{x^2-y^2}$ -wave component. In addition, we argue that they demonstrate that the interlayer tunneling across untwisted layers in single crystal BSCCO is entirely *incoherent*, with no amount of forward scattering. We propose a new type of tricrystal experiment using single crystal *c*-axis twist junctions, that does not employ substrate grain boundaries.

74.50.+r, 74.80.Dm, 74.72.Hs, 74.60.Jg

I. INTRODUCTION

There have been some exciting new developments which reopen the question of the symmetry of the order parameter (OP) in the high temperature superconducting compounds (HTSC). [1–6] Although previous experiments such as the penetration depth, [7] and “phase-sensitive” tricrystal experiments were interpreted as giving strong evidence for an OP in YBa₂Cu₃O_{7-δ} (YBCO) that was dominated at low temperature T by a component of $d_{x^2-y^2}$ symmetry, [8] other experiments showed that there was also a substantial *s*-wave component in that material as well, [9,10] and a very recent experiment suggested a nodeless OP. [5] However, as discussed in the following, the crystal symmetry of YBCO is orthorhombic, with distinct Cu-O bond lengths a and b within the CuO₂ planes, which are normal to and along the CuO chain direction, respectively. This particular type of orthorhombicity then allows for an arbitrary mixing of $d_{x^2-y^2}$ - and *s*-wave OP components, even at T_c . [10,5]

To date, the only hole-doped cuprate superconducting material known to have a consistently tetragonal crystal structure is HgBa₂CuO_{4+δ} (Hg1201). Unfortunately, no “phase-sensitive” experiments have yet been performed on this material. The only experiment relevant to the symmetry of the OP was point contact tunneling, which appeared consistent with an *s*-wave OP at

low T . [11] A material which can sometimes be made in a tetragonal structure is Tl₂Ba₂CuO_{4+δ} (Tl2201). Point contact tunneling and Raman scattering on Tl2201 appeared to be consistent with line nodes of the OP, as expected for a $d_{x^2-y^2}$ -wave OP. [12,13] There was one phase-sensitive experiment performed on Tl2201, which claimed to give strong evidence for a $d_{x^2-y^2}$ -wave OP in that material at low T . [14]. However, Tl2201 is difficult to prepare in the tetragonal form, and most samples of it are actually orthorhombic, in a form similar to that of YBCO. [15] The electron-doped cuprate Nd_{2-x}Ce_xCuO_{4-δ} (NCCO) is also tetragonal, and microwave experiments suggested a full BCS-like gap, [16] suggestive of conventional *s*-wave superconductivity in that material. However, new Pb/NCCO *c*-axis Josephson tunneling experiments demonstrate a surprising small *s*-wave OP component, and no evidence of a gap, suggesting that the full OP might not be pure *s*-wave. [6]

With regards to Bi₂Sr₂CaCu₂O_{8+δ}, (BSCCO), recent phase-sensitive tricrystal experiments also provided evidence at the tricrystal intersection point for a half-integral flux quantum $\Phi_0/2$, where the standard superconducting quantum of flux is $\Phi_0 = hc/2e$. [17] In addition, angle-resolved photoemission spectroscopy (ARPES), penetration depth measurements, point contact tunneling measurements, and Raman scattering experiments were all interpreted as providing additional evidence for a superconducting OP consistent with $d_{x^2-y^2}$

symmetry, although such non-phase-sensitive experiments could only detect the magnitude of the OP. [18–22]

Early attempts to observe c -axis Josephson tunneling between Pb and BSCCO were unsuccessful. [23]. Those experimenters prepared thin films of BSCCO, and deposited a thick layer (roughly 1000Å) of Ag on top of it, followed by a thicker layer of Pb. However, new c -axis Josephson tunneling between Pb and BSCCO provided compelling evidence for a small s -wave OP component at low T . [4] These experimenters cleaved a single crystal of BSCCO, and deposited only about 10Å of Ag on it prior to depositing Pb. The product of the c -axis superconducting critical current I_c and the quasiparticle resistance R_n was found to be very small, about 1-2 μV , curiously about the same as for the new Pb/NCCO junctions. [6] Nevertheless, this evidence for (at least) a small s -wave OP component in BSCCO at low T is very interesting, since BSCCO is orthorhombic in a different sense than is YBCO. As discussed in the following, this form of orthorhombicity does *not* allow for a mixing of $d_{x^2-y^2}$ - and s -wave symmetry at T_c . Thus, these c -axis Pb/BSCCO Josephson experiments could only be explained in the “ d -wave scenario” (in which the purported $d_{x^2-y^2}$ -wave OP component were dominant at T_c) by the appearance of a second phase transition in BSCCO between the T_c values of BSCCO and Pb. The same argument would of course apply to the d -wave scenario as an explanation of the new Pb/NCCO experiments. [6]

Furthermore, c -axis twist experiments have been performed, in which a single crystal of BSCCO was cleaved in the ab -plane, the two single crystal pieces twisted an angle ϕ_0 with respect to each other, and fused together just below the melting temperature. [1–3] Preliminary experiments performed at low T and large magnetic fields $\mathbf{H}||\hat{c}$ showed that the measured I_c across the twist junction did not depend upon ϕ_0 . [1] However, these early results could be interpreted in terms of a dominant $d_{x^2-y^2}$ -wave OP component that could “twist” by mixing in a subdominant d_{xy} -wave OP component. [24] In the vicinity of a 45° twist junction, the dominant $d_{x^2-y^2}$ -wave OP component would be suppressed, allowing the subdominant d_{xy} -wave OP component to become non-vanishing well above T_{c2} , even extending to some extent up to T_c . Thus, one could have a rather ϕ_0 -independent $I_c(\phi_0)$ behavior in the vicinity of the measurement $T = 10$ K, as observed. [1] However, such a scenario would necessarily *also* imply a second bulk phase transition at $T_{c2} \ll T_c$, below which the d_{xy} -wave form could appear. T_{c2} would have to be very low (*i. e.*, $T_{c2} < 1\text{K}$) in the bulk of the sample, if the states in the superconducting “gap” evident at low T were correctly interpreted as arising from nodes in the purported $d_{x^2-y^2}$ -wave OP. [18–22] In addition, although such a scenario could lead to a non-vanishing $I_c(\phi_0 = 45^\circ)$ in the vicinity of T_c , it could not lead to an isotropic $I_c(\phi_0)$ near to T_c .

Now the c -axis twist experiments have been performed

just below T_c in BSCCO. [2,3] These new experiments *also* show no ϕ_0 dependence of $I_c(\phi_0)$. In these experiments, I_c was found to scale with the twist junction area, indicating uniform junctions, and the critical current density J_c^J of the twist junctions was found to be the same as J_c^S , the critical current density for the constituent single crystals, regardless of ϕ_0 . Since BSCCO is intrinsically a stack of Josephson junctions, [25] these experiments demonstrate that the twist junctions behave precisely as the Josephson junctions intrinsic to single crystal BSCCO. Based upon our earlier detailed calculations, these experiments are incompatible with the “ d -wave scenario.” [24] Here, we present general arguments, based solely upon the crystal symmetry, which demonstrate the basic incompatibility of a $d_{x^2-y^2}$ -wave with an s -wave OP component. As shown in the following, the experiments of Li *et al.* provide strong evidence that the OP in BSCCO contains the s -wave component at T_c . We employ group theory to argue that this experiment demonstrates that the dominant OP at T_c contains the s -wave component, but not the purported $d_{x^2-y^2}$ -wave component. These new phase-sensitive experiments are thus in direct contradiction with the phase-sensitive tricrystal experiments of Tsuei and Kirtley *et al.*, which were claimed to provide strong evidence for a dominant $d_{x^2-y^2}$ -wave OP in BSCCO at low T . [17]

II. CRYSTAL SYMMETRIES

Most workers in the field of HTSC agree that the superconducting properties of the materials are determined by the structure of the CuO_2 planes. This is because the electronic structure calculations indicate that the CuO_2 plane bands cross the Fermi energy E_F , [26] and ARPES measurements well above T_c provide strong support for these results. [27] Within the CuO_2 planes, the Cu and O ions are situated approximately as pictured in Fig. 1a. [28] The Cu ions are located on a square lattice, with O ions between near-neighbor Cu ions.

If one ignores the complications of c -axis variations in the relative orientations of different CuO_2 planes, the crystal point group describing a single, tetragonal, CuO_2 plane is C_{4v} . [29–33] The C_{4v} group symmetry operations are indicated in Fig. 1b. In addition to the identity operation E , there are mirror reflections σ_x and σ_y in the planes normal to the layers and containing the x and y axes, respectively, mirror reflections σ_{d1} and σ_{d2} in the planes normal to the layers and containing the diagonals d_1 and d_2 , respectively, and rotations C_4 , C_4^{-1} , and $C_2 = C_4^2$ by 90°, -90°, and 180° about the c -axis, respectively. Tinkham used the slightly different notation σ_v , σ'_v , σ_d , and σ'_d , for the four mirror reflections, respectively. [29] This crystal symmetry is appropriate for Hg1201, NCCO, and for tetragonal samples of Tl2201. [32]

In YBCO, there is an orthorhombic distortion involving the CuO chains, which causes the CuO₂ crystal structure to be longer along the b - (or y -) axis than along the a - (or x -) axis. The crystal space group is $Pmmm$, with the point group of the CuO₂ planes being C_{2v}^1 , an example of C_{2v} . For this lower symmetry, the allowable group operations in addition to E are only σ_x , σ_y , and C_2 , as sketched in Fig. 1c. This group is also appropriate for the double chain compound YBa₂Cu₄O₈ (Y124). However, there are some interesting distortions, which complicate this structure. These are the buckling of the CuO₂ planes along the c -axis direction. [31] Nevertheless, there isn't any buckling within the CuO₂ planes, so it doesn't affect the symmetry arguments relevant to the CuO₂ planes.

In order to correctly interpret the new experiments on BSCCO, it is imperative that the crystal symmetry be understood as thoroughly as possible. The discussion of the symmetry of the superconducting OP in this paper depends crucially upon the notion that there is at least one mirror plane that intersects the CuO₂ plane. This mirror plane then distinguishes OP basis functions that are odd or even with respect to reflections in it. As discussed in the following, the bc -plane is a strict crystallographic mirror plane in most samples.

For overdoped or optimally doped BSCCO, the crystal structure is also orthorhombic, but in this case the inequivalent a - and b -axes are not along the Cu-O bond directions, but along the directions \mathbf{d}_1 and \mathbf{d}_2 diagonal to them. In addition, there is a periodic lattice distortion \mathbf{Q} along one of these diagonals, which we identify as the b - (or d_2 -) axis, consistent with the identification of most workers, [34,35] although some workers identified \mathbf{Q} as being along the a - (or d_1 -) axis direction. [36,37] More precisely, \mathbf{Q} is incommensurate along the reciprocal lattice wavevector \mathbf{b}^* , but commensurate in the other crystal directions, $\mathbf{Q} = (0, 0.212, 1)$. [34–37] The fact that there is a non-vanishing commensurate c -axis component actually removes the σ_{d1} mirror plane crystal symmetry, consistent with the appearance of weak (100) reflections in the x-ray diffraction data. [35,36]. In addition, there is some dispute as to the precise details of the periodic lattice distortion. An early electron diffraction study of BSCCO indicated that in one sample, $\mathbf{Q} = (0.004, 0.212, 1)$, containing a small \mathbf{a}^* component that would also remove the σ_{d2} mirror plane symmetry, [34] although this slight \mathbf{a}^* component of \mathbf{Q} was not seen in high resolution x-ray diffraction experiments on related samples. [34] More to the point, electron diffraction studies of the samples used in the present c -axis twist experiments demonstrated that the small \mathbf{a}^* component of \mathbf{Q} was absent in 90% of the samples. [38] Thus, it appears that although the crystal symmetry of BSCCO is lower than orthorhombic, as the mirror plane σ_{d1} is not precise, most presently-made BSCCO samples exhibit the σ_{d2} mirror plane (the bc -plane). Further experiments to clarify this situation are under way. [38]

This periodic lattice distortion also gives rise to some buckling of the lattice, including Cu-O bond buckling in the bc -plane. Both x-ray studies of the crystal structure of BSCCO used a four-dimensional analysis procedure, and listed the basic space group as $Bb2b$ (or equivalently, $A2aa$), which is the orthorhombic point group C_{2v}^{13} , another form of C_{2v} . [34–37] Unfortunately, they differ slightly in listing the full crystal group as $M : A2aa : \bar{1}11$ and N_{111}^{Bb2b} , respectively. In addition, there is a further complication in some heavily underdoped samples, in that they appear to undergo a phase transition from orthorhombic to monoclinic. [39,40] In such cases, there are no mirror planes (other than parallel to the ab -plane) remaining, and the only non-trivial group operation appropriate for a single CuO₂ plane would be C_2 . However, since the c -axis twist experiments did not involve such monoclinic single crystals, [1,38] we shall not discuss such very low symmetry cases further.

Neglecting these fine details, the allowed symmetry operations of the simplified point group C_{2v}^{13} are E , σ_{d1} , σ_{d2} , and C_2 , as illustrated in Fig. 1d. This symmetry is also appropriate for the compound La_{2-x}Sr_xCuO_{4+δ} (LSCO). With regard to a single CuO₂ layer, the σ_{d1} mirror-plane symmetry is strict, as it is only broken by the c -axis component of \mathbf{Q} in BSCCO. More important, C_{2v}^1 (for YBCO) and C_{2v}^{13} (for BSCCO) differ only in that the in-plane crystal axes are effectively rotated by 45° about the c -axis from each other. As regards the orbital symmetry of the superconducting OP, this difference is *crucial*, as noted in detail below.

III. ORDER PARAMETER COMPONENTS

The role of symmetry upon the OP components in the HTSC was discussed in a recent review article by Annett, Goldenfeld, and Leggett (AGL). [32] However, the notation used by AGL was rather confusing, such as using “ s^- ” to denote a state that contains no s -wave component, and whose leading term is g -wave. More important, the question of whether different OP components could mix with or without a second phase transition was stated incorrectly in the conclusion. Therefore, as the symmetry of the OP in the HTSC is still very much under debate, it is imperative to provide a clear discussion of the issues.

Quantum mechanics, Bloch's theorem, and group theory dictate that the superconducting OP must be consistent with the crystal structure. [29,32] Assuming that the CuO₂ planes are responsible for the superconductivity in the HTSC, then the point group structure of the CuO₂ planes will identify those OP components that are compatible or incompatible with each other. For a tetragonal crystal of Hg1201 or NCCO, these OP components act under the point group C_{4v} according to Table I. The OP components fall into sets, each of which has the same set of eigenvalues in the table. Each set of OP components

with the same eigenvalues under the group operations forms a basis, from which an OP eigenfunction can be constructed. We have labeled these OP eigenfunctions as $|s\rangle$, $|d_{x^2-y^2}\rangle$, $|d_{xy}\rangle$, $|g_{xy(x^2-y^2)}\rangle$, and $|(p_x, p_y)\rangle$, respectively. We have also listed the standard group theoretic (GT) notation for each OP basis set. [29] The spin singlet OPs have one-dimensional representations, with eigenvalue +1 under E . Those labeled A and B are even and odd under C_4 , respectively, and those with subscripts 1 and 2 are even and odd under σ_x and σ_y . Spin triplet OPs have two-dimensional representations, with eigenvalue +2 under the identity operation E , and thus have GT notation E . [29,32,41]

But, how can we best represent the OP basis sets mathematically? We shall employ two methods. In the usual BCS theory, pairing occurs between otherwise free quasiparticles with opposite momenta $\pm\mathbf{k}_F$ on the Fermi surface. For a free-particle Fermi surface, the momenta are then described by the planar angle $\phi_{\mathbf{k}}$, where $\mathbf{k}_F = k_F(\cos\phi_{\mathbf{k}}, \sin\phi_{\mathbf{k}})$. The OP basis is then described as in scattering theory, in which the scattered waves are expanded in terms of angular momentum quantum numbers ℓ . On the other hand, for real-space pairing, the pairing takes place between quasiparticles on distinct lattice sites, such as on the same or nearest-neighbor sites. One then writes $\mathbf{k} = (k_x, k_y)$, which components may satisfy a relation on the real-space Fermi surface. The first Brillouin zone (BZ) is given by $|k_x|, |k_y| \leq \pi/a$. The real-space quantum numbers, (n, m) , count the lattice separations between the paired quasiparticles along the Cu-O bond directions.

In either scenario there are an infinite number of possible OP basis elements, since ℓ is any integer satisfying $\ell \geq 0$ and n, m can be any integers. However, the crystal symmetry forces the infinite number of OP basis elements to appear together in a limited, finite number of OP basis sets, each set having an infinite number of elements. We thus describe each possible OP as having a set of components, each component represented by a basis element. Each element in the OP basis set transforms identically under each of the allowed crystal point group operations.

In the angular momentum ℓ representation, each OP basis function (component) may be written as either $\cos(\ell\phi_{\mathbf{k}})$ or $\sin(\ell\phi_{\mathbf{k}})$. In Fig. 2, we sketch the even ℓ OP basis functions for $\ell \leq 4$ appropriate for singlet spin pairing. Shaded and unshaded regions describe opposite signs of the function. Shown are representations of the $\ell = 0$ s -wave function, a constant, the two $\ell = 2$ functions $d_{x^2-y^2}$ and d_{xy} , proportional to $\cos(2\phi_{\mathbf{k}})$ and $\sin(2\phi_{\mathbf{k}})$, respectively, and the two $\ell = 4$ functions $g_{x^2y^2}$ and $g_{xy(x^2-y^2)}$, proportional to $\cos(4\phi_{\mathbf{k}})$ and $\sin(4\phi_{\mathbf{k}})$, respectively.

GT	OP	E	σ_x	σ_{d1}	C_4	C_2
	Eigenfunction		σ_y	σ_{d2}	C_4^{-1}	
A_1	$ s\rangle$	+1	+1	+1	+1	+1
B_1	$ d_{x^2-y^2}\rangle$	+1	+1	-1	-1	+1
B_2	$ d_{xy}\rangle$	+1	-1	+1	-1	+1
A_2	$ g_{xy(x^2-y^2)}\rangle$	+1	-1	-1	+1	+1
E	$ (p_x, p_y)\rangle$	+2	0	0	0	-2

TABLE I. Superconducting OP character table for a tetragonal crystal such as Hg1201, with point group C_{4v} . The symmetry operations are the identity (E), reflections about the x (σ_x), y (σ_y), d_1 (σ_{d1}), d_2 (σ_{d2}) axes, and rotations about the c -axis by $\pm 90^\circ$ (C_4, C_4^{-1}) and 180° (C_2). The group theoretic (GT) notations A_1, A_2, B_1 , and B_2 are one-dimensional representations, and E is a two-dimensional representation.

The symmetry operations of group C_{4v} (Table I) divide the even ℓ OPs into four basis sets, which are listed in Table II. These sets consist of the basis functions $\cos(\ell\phi_{\mathbf{k}})$ and $\sin(\ell\phi_{\mathbf{k}})$, where ℓ is even, and either is or is not divisible by 4, as indicated in Table II. Thus, the $g_{x^2y^2}$ function, $\cos(4\phi_{\mathbf{k}})$ (equivalent to $1 - 8\hat{k}_x^2\hat{k}_y^2$, which averages to zero), is an element of the same OP basis set ($|s\rangle$) as the $\ell = 0$, s -wave function, a constant. It is possible to define general s -wave eigenfunctions, $\Gamma_i(\phi_{\mathbf{k}}) = \sum_{n=0}^{\infty} A_n^i \cos(4n\phi_{\mathbf{k}})$, each of which transforms as the basis set denoted A_1 in Table I. We are then able to rewrite each of the OP eigenfunctions in terms of the lowest ℓ basis functions multiplying one of these generalized s -wave eigenfunctions, as shown explicitly in Table II.

OP Eigenfunction	ℓ Representation
$ s\rangle$	$\Gamma_1(\phi_{\mathbf{k}})$ $= a_0 + \sqrt{2} \sum_{n=1}^{\infty} a_n \cos(4n\phi_{\mathbf{k}})$
$ d_{x^2-y^2}\rangle$	$\cos(2\phi_{\mathbf{k}})\Gamma_2(\phi_{\mathbf{k}})$ $= \sqrt{2} \sum_{n=1}^{\infty} b_n \cos[(4n-2)\phi_{\mathbf{k}}]$
$ d_{xy}\rangle$	$\sin(2\phi_{\mathbf{k}})\Gamma_3(\phi_{\mathbf{k}})$ $= \sqrt{2} \sum_{n=1}^{\infty} c_n \sin[(4n-2)\phi_{\mathbf{k}}]$
$ g_{xy(x^2-y^2)}\rangle$	$\sin(4\phi_{\mathbf{k}})\Gamma_4(\phi_{\mathbf{k}})$ $= \sqrt{2} \sum_{n=1}^{\infty} d_n \sin(4n\phi_{\mathbf{k}})$

TABLE II. Angular momentum quantum number ℓ representations of the singlet superconducting OP eigenfunctions for a tetragonal crystal. The functions $\Gamma_i(\phi_{\mathbf{k}}) = \sum_{n=0}^{\infty} A_n^i \cos(4n\phi_{\mathbf{k}})$.

In the lattice representation, the general tetragonal eigenfunctions are $\cos[a(nk_x + mk_y)]$ and $\sin[a(nk_x + mk_y)]$, where n and m can be any integers. One classifies the OP basis functions in terms of the spatial separations of the paired quasiparticles. In order of increasing separation, there is on-site (for a retarded BCS-type interaction), near-neighbor, next-nearest-neighbor, etc. pairing. Such expansions of the OP eigenfunctions are presented in Table III. In this representation, the most general OP eigenfunctions in the same basis set as the constant, s -wave OP component can be written as $\tilde{\Gamma}_i(\mathbf{k}) = \sum_{n,m=-\infty}^{\infty} \tilde{A}_{nm}^i \cos[a(nk_x + mk_y)]$, provided that we choose the \tilde{A}_{nm}^i to satisfy the A_1 (s -wave) symmetry, $\tilde{A}_{nm}^i = \tilde{A}_{-n,m}^i = \tilde{A}_{n,-m}^i = \tilde{A}_{-n,-m}^i = \tilde{A}_{mn}^i$, of the C_{4v} character table (Table I). As for the angular momentum representation, it is then possible to write each OP eigenfunction in terms of the nearest pairing separations consistent with the representation group symmetry, multiplied by one of the allowed generalized s -wave lattice eigenfunctions.

OP Eigenfunction	Crystal Representation
$ s\rangle$	$\tilde{\Gamma}_1(\mathbf{k})$ $= \sum_{n,m=0}^{\infty} a_{nm} [\cos(nk_x a) \cos(mk_y a)$ $+ \cos(mk_x a) \cos(nk_y a)]$
$ d_{x^2-y^2}\rangle$	$[\cos(k_x a) - \cos(k_y a)]\tilde{\Gamma}_2(\mathbf{k})$ $= \sum_{n,m=0}^{\infty} b_{nm} [\cos(nk_x a) \cos(mk_y a)$ $- \cos(mk_x a) \cos(nk_y a)]$
$ d_{xy}\rangle$	$\sin(k_x a) \sin(k_y a)\tilde{\Gamma}_3(\mathbf{k})$ $= \sum_{n,m=1}^{\infty} c_{nm} [\sin(nk_x a) \sin(mk_y a)$ $+ \sin(mk_x a) \sin(nk_y a)]$
$ g_{xy(x^2-y^2)}\rangle$	$\sin(k_x a) \sin(k_y a)$ $\times [\cos(k_x a) - \cos(k_y a)]\tilde{\Gamma}_4(\mathbf{k})$ $= \sum_{n,m=1}^{\infty} d_{nm} [\sin(nk_x a) \sin(mk_y a)$ $- \sin(mk_x a) \sin(nk_y a)]$

TABLE III. Lattice representations of the singlet superconducting OP eigenfunctions for a tetragonal crystal. The functions $\tilde{\Gamma}_i(\mathbf{k}) = \sum_{n,m=-\infty}^{\infty} \tilde{A}_{nm}^i \cos[a(nk_x + mk_y)]$, where $\tilde{A}_{nm}^i = \tilde{A}_{-n,m}^i = \tilde{A}_{n,-m}^i = \tilde{A}_{-n,-m}^i = \tilde{A}_{mn}^i$.

Those OP components (or basis functions) within the same basis set, which have the same eigenvalues in the group character table, are *compatible*, and can in principle mix freely, the actual mixing amount depending upon the particular pairing interaction form. OP components arising from different basis sets, with one or more different eigenvalues in the group character table are *incompatible*, and do not ordinarily mix. Each OP eigenfunction is a linear combination of all of the compatible OP basis functions within the same basis set. For tetragonal crystals, the OP eigenfunctions are listed in Tables II and III.

In Table IV, we list the spin-singlet character table and group theoretic notation for the C_{2v} group operations for the orthorhombic crystal structure appropriate for YBCO and Y124. [29] We also listed the angular momentum (ℓ) and lattice (n, m) representations of the two OP eigenfunctions, $|s + d_{x^2-y^2}\rangle$ and $|d_{xy} + g_{xy(x^2-y^2)}\rangle$. Each of these OP eigenfunctions contains two basis sets of the tetragonal OP eigenfunctions in Tables II or III. Thus, $|s + d_{x^2-y^2}\rangle$ contains an arbitrary mixing of the tetragonal $|s\rangle$ and $|d_{x^2-y^2}\rangle$ OP eigenfunctions, for example.

GT	OP Eigenfunction	E	σ_x (σ_a)	σ_y (σ_b)	C_2
A_1	$ s + d_{x^2-y^2}\rangle$ $\xrightarrow{\ell} \tilde{a}_0 + \sqrt{2} \sum_{n=1}^{\infty} [\tilde{a}_n \times$ $\times \cos(2n\phi_{\mathbf{k}})]$ $\xrightarrow{n,m} \sum_{n,m=0}^{\infty} [\tilde{a}_{nm} \times$ $\times \cos(nk_x a) \cos(mk_y a)]$	+1	+1	+1	+1
A_2	$ d_{xy} + g_{xy(x^2-y^2)}\rangle$ $\xrightarrow{\ell} \sqrt{2} \sum_{n=1}^{\infty} [\tilde{b}_n \times$ $\times \sin(2n\phi_{\mathbf{k}})]$ $\xrightarrow{n,m} \sum_{n,m=1}^{\infty} [\tilde{b}_{nm} \times$ $\times \sin(nk_x a) \sin(mk_y a)]$	+1	-1	-1	+1

TABLE IV. Singlet superconducting OP eigenfunctions in the angular momentum (ℓ) and lattice (n, m) representations, their group theoretic notations, and character table for the orthorhombic point group C_{2v} in the form appropriate for YBCO.

We remark that even with only a slight (about 2%) crystallographic difference between the a and b axes in YBCO, the mixing of OP components that would have been in different representations (or basis sets) of the tetragonal group C_{4v} , can be very substantial. For example, there could be a very large mixing of s -wave and $d_{x^2-y^2}$ -wave OP components in YBCO. Especially as the penetration depth within the ab -planes measured in YBCO is anisotropic by about a factor of 2, [7] and the c -axis Josephson tunneling between untwinned YBCO and Pb reproducibly gave values of 1.5 mV, [9] about 25% of the expected result of Ambegaokar-Baratoff, [42], one expects the isotropic $\ell = 0$ OP component to be at least 25% of the maximum OP amplitude at low T . Of course, the penetration depth anisotropy is easiest to understand by accounting for the quasi-one-dimensional Fermi surface of the CuO chains.

GT	OP Eigenfunction	E	σ_{d1} (σ_a)	σ_{d2} (σ_b)	C_2
A_1	$ s + d_{xy}\rangle$ $\xrightarrow{\ell} \tilde{a}_0 + \sqrt{2} \sum_{n=1}^{\infty} \{ \tilde{a}_n \times$ $\quad \times \cos[2n(\phi_{\mathbf{k}} - \pi/4)] \}$ $\xrightarrow{n,m} \sum_{n,m=0}^{\infty} \{ [\tilde{a}_{nm} + \tilde{a}_{mn}] \times$ $\quad \times \cos(nk_x a) \cos(mk_y a)$ $\quad + [\tilde{c}_{nm} + \tilde{c}_{mn}] \times$ $\quad \times \sin(nk_x a) \sin(mk_y a) \}$	+1	+1	+1	+1
A_2	$ d_{x^2-y^2} + g_{xy}(x^2-y^2)\rangle$ $\xrightarrow{\ell} \sqrt{2} \sum_{n=1}^{\infty} \{ \tilde{b}_n \times$ $\quad \times \sin[2n(\phi_{\mathbf{k}} - \pi/4)] \}$ $\xrightarrow{n,m} \sum_{n,m=0}^{\infty} \{ [\tilde{a}_{nm} - \tilde{a}_{mn}] \times$ $\quad \times \cos(nk_x a) \cos(mk_y a)$ $\quad + [\tilde{c}_{nm} - \tilde{c}_{mn}] \times$ $\quad \times \sin(nk_x a) \sin(mk_y a) \}$	+1	-1	-1	+1

TABLE V. Singlet superconducting OP eigenfunctions in the angular momentum (ℓ) and lattice (n, m) representations, their group theoretic notations, and character table for the orthorhombic point group C_{2v} in the form appropriate for BSCCO. Although the σ_{d1} mirror plane symmetry is only approximate due to the c -axis component of \mathbf{Q} , the σ_{d2} mirror plane symmetry is robust in most current samples.

In Table V, we list the spin-singlet character table and group theoretic notation for the C_{2v} orthorhombic group operations appropriate for BSCCO and LSCO. We also listed the angular momentum (ℓ) and lattice (n, m) representations of the two OP eigenfunctions, $|s + d_{xy}\rangle$ and $|d_{x^2-y^2} + g_{xy}(x^2-y^2)\rangle$. Each of these OP eigenfunctions contains two basis sets of the tetragonal OP eigenfunctions in Tables II or III. Thus, $|s + d_{xy}\rangle$ contains an arbitrary mixing of the tetragonal $|s\rangle$ and $|d_{xy}\rangle$ OP eigenfunctions, but not of the tetragonal $|d_{x^2-y^2}\rangle$ OP eigenfunction. We note that although the ac -plane is not a strict BSCCO crystallographic mirror plane, the bc -plane is a strict crystallographic mirror plane (σ_{d2}). This fact is sufficient to separate the OP sets as if the crystal were fully orthorhombic.

We remind the reader of the crucial difference between the OPs with the same group theoretic notations for the orthorhombic symmetries appropriate for YBCO and BSCCO, respectively. Although for orthorhombic YBCO, OP components that have s -wave and $d_{x^2-y^2}$ -wave symmetry in the tetragonal crystal can mix freely, and similarly OP components exhibiting d_{xy} -wave and $g_{xy}(x^2-y^2)$ -wave symmetry in the tetragonal crystal can mix, in BSCCO this is not the case. Instead, the OP components exhibiting $d_{x^2-y^2}$ -wave and $g_{xy}(x^2-y^2)$ -wave symmetry in the tetragonal crystal can mix, as can the OP components having s -wave and d_{xy} -wave symmetry in the tetragonal crystal representation.

IV. GINZBURG-LANDAU FREE ENERGY

In this section, we examine the Ginzburg-Landau free energy of a superconductor with one or more OP components. We limit our discussion to a single CuO₂ layer, assuming equivalent OPs on all CuO₂ layers. We shall see that there is a distinct difference between the cases of two *compatible* OP components and two *incompatible* OP components. (AGL used the terminology “mixing” and “non-mixing”).

A. single complex OP component

We first assume a single OP component. Let the pairing interaction $\lambda(\mathbf{k}, \mathbf{k}') = \lambda_0 \varphi(\mathbf{k}) \varphi(\mathbf{k}')$, where the basis function $\varphi(\mathbf{k})$ is normalized, *i. e.*, $\langle \varphi(\mathbf{k}) | \varphi(\mathbf{k}) \rangle = 1$, which in angular momentum representation implies $\int_0^{2\pi} \frac{d\phi_{\mathbf{k}}}{2\pi} \varphi^2(\phi_{\mathbf{k}}) = 1$, or in real-space representation implies $(a/2\pi)^2 \int_{-\pi/a}^{\pi/a} dk_x \int_{-\pi/a}^{\pi/a} dk_y \varphi^2(\mathbf{k}) = 1$, and the OP eigenfunction $\Delta(\mathbf{k}, T) = \Delta(T) \varphi(\mathbf{k})$, where $\Delta(T)$ is the OP amplitude. The Ginzburg-Landau free energy of a spatially and temporally uniform superconductor with a single OP component is

$$F = \alpha(T) |\Delta(T)|^2 + \beta |\Delta(T)|^4, \quad (1)$$

where $\alpha(T) = \alpha_0(T - T_c)$, $\beta > 0$ is a constant, and T_c is obtained from λ_0 in the usual BCS approximation. Minimizing F , we find $\Delta = 0$ and $F_N = 0$ for $T \geq T_c$, and $\Delta(T) = [\alpha_0(T_c - T)/(2\beta)]^{1/2}$ and $F_S = -\alpha_0^2(T_c - T)^2/(4\beta)$ for $T < T_c$.

B. Two incompatible OP components

We now consider the case of two incompatible OP components. For simplicity, we consider the case in which the pairing interaction can be written in terms of products of only two of the incompatible, orthonormal basis functions $\varphi_i(\mathbf{k})$ appropriate for the crystal, $\lambda(\mathbf{k}, \mathbf{k}') = \sum_{i=1}^2 \lambda_{i0} \varphi_i(\mathbf{k}) \varphi_i(\mathbf{k}')$. As examples of incompatible basis functions, in Hg1201, YBCO, or BSCCO, we could choose the simplest d_{xy} -wave and $d_{x^2-y^2}$ -wave basis functions, which are $\sqrt{2} \sin(2\phi_{\mathbf{k}})$ and $\sqrt{2} \cos(2\phi_{\mathbf{k}})$ in the ℓ -representation. For either Hg1201 or YBCO, we could also choose the simplest s -wave and d_{xy} -wave functions (1 and $\sqrt{2} \sin(2\phi_{\mathbf{k}})$ in the ℓ -representation), and for either Hg1201 or BSCCO, we could also choose the simplest s -wave and $d_{x^2-y^2}$ -wave basis functions. Of course, the number of possible incompatible OP component pairs is limitless. The OP eigenfunction consistent with the above pairing interaction has the form $\Delta(\mathbf{k}, T) = \sum_{i=1}^2 \Delta_i(T) \varphi_i(\mathbf{k})$, where the $\Delta_i(T)$ are complex constants representing the two incompatible OP component amplitudes.

For different λ_{i0} , the bare transition temperatures T_{ci} (obtained in the BCS model assuming only one $\Delta_i \neq 0$) of the two incompatible components are different. The free energy can then be written as

$$F = \sum_{i=1}^2 \left(\alpha_i(T) |\Delta_i|^2 + \beta_i |\Delta_i|^4 \right) + \epsilon |\Delta_1|^2 |\Delta_2|^2 + \delta [\Delta_1^2 \Delta_2^{*2} + \Delta_2^2 \Delta_1^{*2}], \quad (2)$$

where the $\alpha_i(T) = \alpha_{i0}(T - T_{ci})$ and the β_i , ϵ and δ are constants. In weak coupling (BCS) theory, $\beta_i > 0$, $\epsilon > 0$, $\delta > 0$, and $\epsilon - 2\delta > 0$. Writing $\Delta_i = |\Delta_i| \exp(i\psi_i)$, we note that the only term depending upon the phases ψ_i is the one proportional to δ , which becomes $2\delta |\Delta_1|^2 |\Delta_2|^2 \cos[2(\psi_1 - \psi_2)]$. Assuming $T_{c1} > T_{c2}$, F is minimized in the first superconducting (S_1) regime just below T_c , by

$$|\Delta_1(T)| = [-\alpha_1(T)/(2\beta_1)]^{1/2}, \\ |\Delta_2| = 0, \quad \text{for } T_{c2}^< \leq T < T_{c1} \quad (S_1). \quad (3)$$

In the low temperature (S_2) superconducting phase, both $|\Delta_1| \neq 0$ and $|\Delta_2| \neq 0$. $\partial F/\partial \psi_i = 0$ is satisfied when $\sin[2(\psi_1 - \psi_2)] = 0$, which minimizes F when $\psi_1 - \psi_2 = \pm\pi/2$. The temperature $T_{c2}^<$ which separates the regions

S_1 from S_2 can then be obtained by inserting $|\Delta_1|$ from Eq. (3) into the linearized equation for $|\Delta_2|$, leading to

$$\frac{T_{c2}^<}{T_{c2}} = \frac{1 - \nu_1(T_{c1}/T_{c2})}{1 - \nu_1}, \\ \nu_1 = \frac{\alpha_{10}(\epsilon - 2\delta)}{2\alpha_{20}\beta_1}. \quad (4)$$

Note that $T_{c2}^< < T_{c2}$ if $\epsilon - 2\delta > 0$, as in weak coupling (BCS) theory. Then, solving a quadratic for $|\Delta_1|^2$ and $|\Delta_2|^2$ below $T_{c2}^<$, we obtain the solution in the low temperature superconducting phase S_2 ,

$$|\Delta_2|^2 = \frac{\alpha_{20}(1 - \nu_1)(T_{c2}^< - T)}{2\beta_2(1 - \nu_1\nu_2)} \\ |\Delta_1|^2 = \frac{\alpha_{10}}{2\beta_1} \left[T_{c1} - T_{c2}^< - \frac{(1 - \nu_2)(T_{c2}^< - T)}{1 - \nu_1\nu_2} \right] \\ \nu_2 = \frac{\alpha_{20}(\epsilon - 2\delta)}{2\alpha_{10}\beta_2} \\ \psi_2 = \psi_1 \pm \pi/2 \quad \text{for } T < T_{c2}^< \quad (S_2). \quad (5)$$

Because of the $\pi/2$ phase difference between the two OP components in the S_2 state, this is commonly known as the “ $\Delta_1 + i\Delta_2$ ” state. As emphasized by AGL, these two (or more) incompatible OP components can only be simultaneously non-vanishing below a second phase transition temperature, $T_{c2}^<$. Since no second phase transition appears to have been observed in any of the cuprates (at least, not above 1 K as yet), it is rather unlikely that $T_{c2}^< > 1$ K. In addition, the $\Delta_1 + i\Delta_2$ states is nodeless below $T_{c2}^<$.

C. Two compatible OP components

Now we consider the more interesting case of two compatible OP components, with elements $\varphi_i(\mathbf{k})$ for $i = 1, 2$, of the same basis set. In Hg1201, for example, $|s\rangle$ contains the simplest s -wave and $g_{x^2y^2}$ -wave elements (written as 1 and $\sqrt{2} \cos(4\phi_{\mathbf{k}})$ in the ℓ -representation), which are compatible basis functions. For YBCO, $|s + d_{x^2-y^2}\rangle$ contains as compatible basis functions the simplest s -wave and $d_{x^2-y^2}$ -wave functions (1 and $\sqrt{2} \cos(2\phi_{\mathbf{k}})$ in the ℓ -representation), and for BSCCO, the simplest s -wave and d_{xy} -wave functions are compatible elements of $|s + d_{xy}\rangle$. It is easy to generalize this procedure to include all of the (infinite number of) components in the relevant basis set.

With two compatible OP components, the interaction is generally of the form $\lambda(\mathbf{k}, \mathbf{k}') = \sum_{i,j=1}^2 \varphi_i(\mathbf{k}) \lambda_{ij0} \varphi_j(\mathbf{k}')$, where $\overset{\leftrightarrow}{\lambda}_0$ is a symmetric tensor of rank 2. We could use this form of $\lambda(\mathbf{k}, \mathbf{k}')$ to generate the Ginzburg-Landau free energy, letting

$\Delta(\mathbf{k}, T) = \sum_{i=1}^2 \Delta_i(T) \varphi_i(\mathbf{k})$, where the Δ_i are complex constants representing the OP component amplitudes. We would then find that the free energy would be given by Eq. (2), plus the terms $\gamma(\Delta_1^* \Delta_2 + \Delta_1 \Delta_2^*)$ and $(\Delta_1 \Delta_2^* + \Delta_1^* \Delta_2)(\mu_1 |\Delta_1|^2 + \mu_2 |\Delta_2|^2)$. [32] In the BCS approximation, the T_{ci} arise from the diagonal elements λ_{ii0} , and γ and the μ_i arise from the off-diagonal $\lambda_{120} = \lambda_{210}$ elements of $\overleftrightarrow{\lambda}_0$, respectively. One could then diagonalize the part of this free energy quadratic in the Δ_i by a unitary transformation, a two-dimensional rotation, as noted by AGL. [32] However, AGL did not emphasize the important point that this rotation *mixes* the OP components for all $T \leq T_c$. In order to clarify this point, we choose instead to first diagonalize the pairing interaction. To do so, we let $\overleftrightarrow{\lambda}_0 = \overleftrightarrow{R} \overleftrightarrow{\lambda}_0 \overleftrightarrow{R}^{-1}$, where \overleftrightarrow{R} is a standard two-dimensional matrix for rotation by an angle θ about the \hat{z} axis. By choosing $\tan(2\theta) = 2\lambda_{120}/(\lambda_{110} - \lambda_{220})$, we obtain the diagonalized $\overleftrightarrow{\lambda}_0$, and the pairing interaction can now be written as $\lambda(\mathbf{k}, \mathbf{k}') = \sum_{S=\pm} \varphi_S(\mathbf{k}) \tilde{\lambda}_{S0} \varphi_S(\mathbf{k}')$, where

$$\begin{aligned} \varphi_+(\mathbf{k}) &= \varphi_1(\mathbf{k}) \cos \theta + \varphi_2(\mathbf{k}) \sin \theta \\ \varphi_-(\mathbf{k}) &= -\varphi_1(\mathbf{k}) \sin \theta + \varphi_2(\mathbf{k}) \cos \theta, \end{aligned} \quad (6)$$

and $\Delta(\mathbf{k}, T) = \sum_{S=\pm} \Delta_S(T) \varphi_S(\mathbf{k})$. We then expand the free energy in powers of Δ_{\pm} , and obtain

$$\begin{aligned} F &= \sum_{S=\pm} \left(\alpha_S(T) |\Delta_S|^2 + \beta_S |\Delta_S|^4 \right) \\ &+ \epsilon |\Delta_+|^2 |\Delta_-|^2 + \delta (\Delta_+^2 \Delta_-^{*2} + \Delta_+^{*2} \Delta_-^2) \\ &+ (\Delta_+ \Delta_-^* + \Delta_- \Delta_+^*) (\mu_+ |\Delta_+|^2 + \mu_- |\Delta_-|^2), \end{aligned} \quad (7)$$

where $\alpha_{\pm}(T) = \alpha_{\pm 0}(T - T_{c\pm})$, $T_{c\pm}$ is obtained from $\tilde{\lambda}_{\pm 0} = \frac{1}{2} \{ \lambda_{110} + \lambda_{220} \pm [(\lambda_{110} - \lambda_{220})^2 + 4\lambda_{210}^2]^{1/2} \}$ in the BCS approximation.

Now, it is evident that the two original OP components Δ_1 and Δ_2 mix in *two* ways. First, and most important, the corresponding basis functions $\varphi_i(\mathbf{k})$ mix via the linear transformation employed to diagonalize the quadratic part of the free energy. Since the transformed OP eigenfunctions are $\Delta_{\pm}(T) \varphi_{\pm}(\mathbf{k})$, *both* transformed OP eigenfunctions contain contributions from *both* compatible basis functions. Thus, the dominant OP Δ_+ (as well as the subdominant Δ_-) could be written as a “ $\Delta_1 + \Delta_2$ ” state. Although AGL did not emphasize it, this mixing does *not* require a second phase transition.

Second, the subdominant OP (with the lower transition temperature, T_{c-}) is coupled to the dominant OP just below T_{c+} via the term $\mu_+ |\Delta_+|^2 (\Delta_+ \Delta_-^* + \Delta_- \Delta_+^*)$. Depending upon the sign of μ_+ , Δ_- will either add or detract from Δ_+ , but in either case, it will be in phase with it. The most important part of the resulting free energy just below T_{c+} is then

$$\begin{aligned} F &\approx -\alpha_+^2(T)/(4\beta_+) + \alpha_-(T) |\Delta_-|^2 \\ &- 2|\mu_+| |\Delta_-| \left[-\alpha_+(T)/(2\beta_+) \right]^{3/2}, \end{aligned} \quad (8)$$

which implies

$$|\Delta_-(T)| \approx \frac{2|\mu_+|}{\alpha_-(T_{c+})} \left(\frac{-\alpha_+(T)}{2\beta_+} \right)^{3/2}, \quad (9)$$

which behaves as $(T_{c+} - T)^{3/2}$. Thus, the subdominant compatible OP can pick up a strong temperature dependence just below T_{c+} , modifying the relative temperature dependences of Δ_1 and Δ_2 in the “ $\Delta_1 + \Delta_2$ ” state. In particular, it is possible for one compatible component, say Δ_2 , to be substantially smaller than the other just below T_c , but comparable to the other at low T . Again, this can occur *without* a second phase transition, a point that was incorrectly stated in the conclusion of AGL.

More generally, when the (symmetric) interaction matrix $\overleftrightarrow{\lambda}_0$ represents pairing involving a large (or infinite) number of compatible basis set elements, one diagonalizes it, and rank orders the diagonalized interaction strengths $\tilde{\lambda}_{ii0}$. Each eigenvalue $\tilde{\lambda}_{ii0}$ corresponds to a bare T_{ci} value, with $T_c = T_{c1}$. Each $\tilde{\lambda}_{ii0}$ also corresponds to an OP eigenfunction which is a large (or infinite) sum of the compatible basis set elements. The resulting free energy will then contain quartic terms that mix two or more OPs. These terms will further mix the OPs, changing their effective T dependences and relative weights below T_c . Thus, the most general OP eigenfunction will have the general form given in Tables II-V, with coefficients (such as the a_n for $|s\rangle$ in Table II) having somewhat different T dependences. This implies that the \mathbf{k} -dependence of the OP eigenfunction changes smoothly with temperature. [43] *None* of this compatible mixing involves a second phase transition.

V. C-AXIS TWIST JOSEPHSON JUNCTIONS

We now consider briefly the case of a HTSC Josephson junction formed by twisting bicrystal halves an angle ϕ_0 about the c -axis, as pictured in Fig. 3. Let us suppose that there is only one phase transition observed in a given material. Certainly in the vicinity of the bulk transition T_c , it is hard to imagine that a transition to a second state with a combined OP that mixes incompatible components would be present, except in the case of the triplet OPs. However, since $|p_x, p_y\rangle$ is a two-dimensional representation of the tetragonal group, it gives rise to a “ $p_x + ip_y$ ” (or equivalently, a “ $p_{d1} + ip_{d2}$ ”) state, as in the equatorial plane of the A phase of He^3 . In an orthorhombic crystal, the transition temperatures T_{c1}, T_{c2} for the two incompatible components are split, and a second phase transition appears at $T_{c2} <$, below which the second component becomes non-vanishing. In

any event, the combined OP eigenfunction will be nodeless and rather isotropic at low T . If this were true, one could not presume that the ARPES, penetration depth, Raman, and tunneling experiments were in any way probing the superconducting OP, so that one would need to explain those and related experiments from a model that did *not* contain any nodes of the OP.

Thus, we assume that we are sufficiently close to T_c so that only one OP eigenfunction with compatible basis elements need be considered. Let there be two crystal half-spaces, which are rotated an angle ϕ_0 with respect to each other. On the upper half-space, we let the OP be $\Delta_U(\phi_{\mathbf{k}} - \phi_0/2)$, and on the lower half-space, it is $\Delta_L(\phi_{\mathbf{k}'} + \phi_0/2)$. We assume that there is sufficient Josephson coupling across the junction for a critical current to traverse it.

As we discussed in detail elsewhere, there are two mechanisms by which quasiparticles can tunnel across the twist boundary. [24] These are *coherent* and *incoherent* tunneling, respectively. In the coherent tunneling process, the momenta parallel to the twist junction are conserved during the tunneling, whereas for incoherent tunneling, they are ordinarily taken to be completely random. We assume that the spatial average of the second order quasiparticle tunneling processes across the twist boundary can be written as

$$\begin{aligned} \langle t(\mathbf{k} - \mathbf{k}')t^*(\mathbf{k}' - \mathbf{k}'') \rangle &= \delta(\mathbf{k} - \mathbf{k}'') [|J|^2 \delta(\mathbf{k} - \mathbf{k}') \\ &+ f_{\text{inc}}(\phi_{\mathbf{k}} - \phi_{\mathbf{k}'}), \end{aligned} \quad (10)$$

where the overall two-dimensional $\delta(\mathbf{k} - \mathbf{k}'')$ function insures translational invariance after averaging. The terms proportional to $|J|^2$ and $f_{\text{inc}}(\phi_{\mathbf{k}} - \phi_{\mathbf{k}'})$ are the coherent and incoherent part of the tunneling. Ordinarily, one expects $f_{\text{inc}}(\phi_{\mathbf{k}} - \phi_{\mathbf{k}'})$ to be a constant, as for the standard s -wave scattering calculation of Ambegaokar-Baratoff. [42] However, to allow for a small amount of forward scattering, or incoherent tunneling of non- s -wave character, we let

$$f_{\text{inc}}(\phi_{\mathbf{k}} - \phi_{\mathbf{k}'}) = \sum_{\ell=0}^{\infty} \frac{\cos[\ell(\phi_{\mathbf{k}} - \phi_{\mathbf{k}'})]}{2\pi\tau_{\perp\ell}N_{2D}(0)}, \quad (11)$$

where $N_{2D}(0) = m/(2\pi)$ is the two-dimensional single-spin quasiparticle density of states. [24]

We remark that the question of coherent versus incoherent tunneling is an interesting one, especially when one considers tunneling between two layers that are twisted about the c -axis with respect to each other. The important point is that a quasiparticle tunnels from the Fermi surface on one layer to the Fermi surface on the neighboring layer. This is true in both the normal and superconducting states. For the simple case of a quasi-two-dimensional free-particle band, the cross-section of the Fermi surface in the k_x/k_y plane is a circle centered

about the high-symmetry Γ point at the center of the first BZ. Even for the case of layers twisted about the c -axis, the circular Fermi surface cross-sections are identical in both first BZs twisted an angle ϕ_0 with respect to each other. In the coherent single particle tunneling process, one can in principle tunnel from one layer to the next from any position within the first BZ, and for such a free particle Fermi surface, coherent normal state quasiparticle tunneling could occur with equal probability over this circular cross-section, even for arbitrary ϕ_0 , as long as the applied voltage V was effectively zero.

In the cuprates, however, the CuO_2 bands generally have the tight-binding, rather than the free-particle form. For BSCCO, the actual Fermi surface is rather complicated, as pictured in Fig. 4a. First of all, the primary Fermi surface is very similar to the tight-binding Fermi surface indicated by the thick curves in Fig. 4a. These curves were calculated using the two-dimensional tight-binding dispersion

$$\begin{aligned} \xi(\mathbf{k}) &= t[\cos(k_x a) + \cos(k_y a)] \\ &- t' \cos(k_x a) \cos(k_y a) - \mu, \end{aligned} \quad (12)$$

where the primary Fermi surface is obtain by setting $\xi(\mathbf{k}_F) = 0$. In Fig. 4a, we used the values $t = 2t' = 0.8\mu$, which gives a primary Fermi surface similar to that calculated for BSCCO and observed in ARPES experiments. [18,26,27] In addition, there are the secondary Fermi surfaces, which arise from the periodic lattice distortion $\mathbf{Q} = (0, 0.212, 1)$ in terms of the reciprocal lattice vectors. [34] These are given by $\xi(\mathbf{k}_F \pm \mathbf{Q}) = 0$, which are indicated by the thin solid and dotted curves in Fig. 4a. Note that for this two-dimensional dispersion, the c -component of \mathbf{Q} is irrelevant to the Fermi surface structure. For c -axis tunneling between adjacent layers that lie directly on top of one another, one could in principle still have coherent tunneling at any position on the multiple Fermi surfaces within the first BZ. When adjacent layers are twisted an angle ϕ_0 about the c -axis with respect to each other, as pictured for $\phi_0 = \pi/4$ in Fig. 4b, however, the Fermi surfaces on adjacent layers intersect only at a finite set of points. This intersection has measure zero relative to the entire length of the two-dimensional Fermi surface. We thus expect the amount of coherent tunneling between layers twisted by a sizable angle ϕ_0 to be vanishingly small. Otherwise, preserving the wavevector during the coherent tunneling process necessarily requires inelastic processes. Thus, except for the cases of $\phi_0 \approx 0, \pi/2$, we expect the dominant interlayer tunneling processes to be *incoherent*.

Previously, [24] we treated the theoretically more interesting (and more complicated) case in which the composition of the OP components can depend upon the layer index, as the twist junction specifically removes translational invariance. For the case in which the dominant

OP component is presumed to be $d_{x^2-y^2}$ -wave and the secondary, incompatible OP component is d_{xy} -wave, the dominant OP component is suppressed by the proximity to the twist junction, locally reducing the suppression of the sub-dominant OP component in the bulk of the sample by the dominant OP component. In addition, for all $T < T_c$, this sub-dominant OP component would be locally enhanced, although the enhancement would become quite weak close to T_c . This would allow the local OP to twist, compensating for the physical twist in the junction, and allowing a finite amount of Josephson critical current at all twist angles.

We found, however, that sufficiently close to the bulk T_c , only one OP component need be considered, except for the special (and only infinitesimally probable) case of an *accidental degeneracy*, whereby two incompatible OPs accidentally happen to have (almost) exactly the same bare transition temperature, and combine to give a nodeless $\Delta_1 + i\Delta_2$ state. [24] Otherwise, assuming the bare T_{cB} of the secondary d_{xy} OP component is sufficiently small that $T_{cB} < T_c$, the suppressed secondary transition in the bulk, is unobservable experimentally, the Josephson coupling strength determines the T at which the OP twisting could occur. The weaker the coupling, the lower the T at which the OP can compensate for the junction twist by OP twisting, and the experiment becomes definitive in the vicinity of T_c . Such effects were shown in Fig. 4b of our earlier paper. [24] In that case, we showed explicitly that for strong ($\eta_d = \eta'_d = 1$) d -wave Josephson coupling across the twist junction (η'_d) and non-junction (η_d) layers, respectively, a small but finite $I_c(\phi_0 = 45^\circ)$ was obtained at $t = T/T_{cA} = 0.7$. However, reducing η'_d to 0.01 dramatically reduced $I_c(\phi_0 = 45^\circ)$ at $t = 0.7$. Moreover, as the experiments of Li *et al.* now indicate that $\eta = \eta' \ll 1$ in BSCCO, we have recalculated $I_c(\phi_0)$ for the cases $\eta_d = \eta'_d = 0.1, 0.001$, and plotted the results for $t = 0.5, 0.9, 0.99$ in Fig. 5. The remaining parameters are the same as before, and are listed in the caption to Fig. 5. It is seen that for $T_{cB}/T_{cA} = 0.2$ (about as high as one could possibly hope to have, in order for quasi-nodes to still be present at 1 K), both sets of curves show the suppression of the dominant OP component near to T_c , with $I_c(\phi_0)/I_c(0)$ lying below $|\cos(2\phi_0)|$ except for $\phi_0 \approx 45^\circ$. They also show that $I_c(\phi_0 = 45^\circ)$ decreases with increasing T/T_{cA} and decreasing $\eta_d = \eta'_d$. Clearly, twisting of the purported d -wave OP *cannot* explain the experiment of Li *et al.*, in which $I_c(\phi_0)$ was found to be independent of ϕ_0 .

We therefore now consider the case in which there is only one OP, but that it may contain a complex mixture of compatible basis set functions. In the Ginzburg-Landau regime near to T_c , we found that the Josephson critical current across the twist junction could be written in terms of coherent and incoherent parts, $I_c^{\text{coh}}(\phi_0, T) + I_c^{\text{inc}}(\phi_0, T)$, [24] where

$$I_c^{\text{coh}}(\phi_0, T) \rightarrow 2eN_{2D}(0)b_0(T)|J|^2 \text{Im} \int_0^{2\pi} d\phi_{\mathbf{k}} \\ \times \Delta_U(\phi_{\mathbf{k}} - \phi_0/2)\Delta_L^*(\phi_{\mathbf{k}} + \phi_0/2)$$

and

$$I_c^{\text{inc}}(\phi_0, T) \rightarrow eN_{2D}^2(0)a_0(T) \text{Im} \int_0^{2\pi} d\phi_{\mathbf{k}} \int_0^{2\pi} d\phi_{\mathbf{k}'} \\ \times \Delta_U(\phi_{\mathbf{k}} - \phi_0/2)f_{\text{inc}}(\phi_{\mathbf{k}} - \phi_{\mathbf{k}'}) \\ \times \Delta_L^*(\phi_{\mathbf{k}'} + \phi_0/2), \quad (13)$$

where $a_0(T) = \pi/(4T)$ and $b_0(T) = 7\zeta(3)/(8\pi^2T^2)$. Near T_c , $I_c(\phi_0, T)$ is proportional to $(T_c - T)$.

We then have to evaluate $I_c(\phi_0)$ for the various OP possibilities for Hg1201, YBCO, and BSCCO. To do so, it is convenient to define

$$\eta_0^{\text{inc}} = e\pi N_{2D}(0)a_0(T)/\tau_{\perp 0} \\ \tilde{\eta}_\ell = \frac{\tau_{\perp 0}}{\tau_{\perp \ell}} + \frac{2b_0(T)|J|^2\tau_{\perp 0}}{a_0(T)}. \quad (14)$$

Clearly, η_0^{inc} is one-half the amplitude of the incoherent scattering contribution to the critical current for the s -wave OP component, and $\tilde{\eta}_\ell$ is a measure of the coherent and incoherent contributions to I_c from the ℓ -wave OP components, relative to that of η_0^{inc} . Note that $\tilde{\eta}_2 \propto \eta'_d$ in Fig. 5.

GT	OP	$I_c(\phi_0)/\eta_0^{\text{inc}}$
A_1	$ s\rangle$	$\left a_0^2 + \sum_{n=0}^{\infty} \tilde{\eta}_{4n} a_n^2 \cos(4n\phi_0) \right $
B_1	$ d_{x^2-y^2}\rangle$	$\left \sum_{n=1}^{\infty} \tilde{\eta}_{4n-2} b_n^2 \cos[(4n-2)\phi_0] \right $
B_2	$ d_{xy}\rangle$	$\left \sum_{n=1}^{\infty} \tilde{\eta}_{4n-2} c_n^2 \cos[(4n-2)\phi_0] \right $
A_2	$ g_{xy(x^2-y^2)}\rangle$	$\left \sum_{n=1}^{\infty} \tilde{\eta}_{4n} d_n^2 \cos(4n\phi_0) \right $

TABLE VI. Superconducting critical current across junctions twisted by ϕ_0 about the c -axis of tetragonal crystals such as Hg1201 (from Table II).

In Table VI, we list the resulting $I_c(\phi_0)/\eta_0^{\text{inc}}$ for the singlet OPs in tetragonal materials such as Hg1201. In Table VII, $I_c(\phi_0)/\eta_0^{\text{inc}}$ is presented for the orthorhombic materials BSCCO and YBCO. We note, however, that in this case the actual forms of the OP eigenfunctions involved in the respective states of those two orthorhombic materials are different, as they are given in Tables IV and V. From Table VI, the generalized d -wave states (with B group theoretic symmetry) are indistinguishable from each other. The leading $\ell = 2$ components of these generalized d -wave states give rise to $I_c(\phi_0 = 45^\circ) = 0$. The leading $\ell = 4$ contribution to the generalized $g_{xy(x^2-y^2)}$ -wave state likewise give rise to $I_c = 0$ at $\phi_0 = \pm 22.5^\circ$ and $\pm 67.5^\circ$. For completeness, the leading $\ell = 1$ triplet OP components give rise to $I_c(\phi_0 = 90^\circ) = 0$. These simple leading ℓ cases give rise to $I_c(\phi_0) \propto |\cos(\ell\phi_0)|$. These simple cases are pictured in Fig. 6.

Including compatible components of higher ℓ values will not change these qualitative results. In addition, if the tunneling across the twist junction is entirely incoherent, with s -wave incoherent tunneling only ($\tau_{\perp\ell} \rightarrow \infty$ for $\ell \neq 0$), then these states will give a vanishing critical current for all twist angles ϕ_0 (even for the untwisted case $\phi_0 = 0$), and the generalized s -wave state would result in a constant $I_c(\phi_0)$, the constant being a measure of the $\ell = 0$, pure s -wave part of the OP eigenfunction.

On the other hand, if the relative contribution of the pure s -wave form to the entire OP eigenfunction were very small (*i. e.*, nearly vanishing), then a more complicated scenario could develop. For instance, if either higher ℓ -incoherent or coherent intertwist tunneling were present and substantial, and if the contribution to the intertwist tunneling arising from the $g_{x^2y^2}$ component were larger than the contribution arising from the s component, and the $\ell \geq 8$ -wave components of the OP vanished, then there could be angles ϕ_0^* satisfying $\phi_0^* = \frac{1}{4} \cos^{-1}[-a_0^2(1 + \tilde{\eta}_0)/\tilde{\eta}_4 a_1^2]$ at which $I_c(\phi_0^*) = 0$. Including higher ℓ components of the generalized s -wave OP could cause the actual ϕ_0^* values to deviate from this simple formula, however, as pictured in Figs. 7a, 7b, and 7c. Such a scenario is mainly expected in the case of a nearly vanishing $\ell = 0$ OP component, since the tunneling at a finite twist angle is most likely incoherent for tight-binding Fermi surfaces.

GT	$I_c(\phi_0)/\eta_0^{\text{inc}}$
A_1	$\left \tilde{a}_0^2(1 + \tilde{\eta}_0) + \sum_{n=1}^{\infty} \tilde{\eta}_{2n} \tilde{a}_n^2 \cos(2n\phi_0) \right $
A_2	$\left \sum_{n=1}^{\infty} \tilde{\eta}_{2n} \tilde{b}_n^2 \cos(2n\phi_0) \right $

TABLE VII. Superconducting critical current across c -axis junctions twisted by ϕ_0 , for orthorhombic YBCO or BSCCO, from Tables IV and V. See text.

For an orthorhombic triplet superconductor, a twist angle of $\pm 90^\circ$ should give rise to a vanishing critical current, as pictured in Fig. 6. This is clearly contradicted by the present experiments on BSCCO of Li *et al.*, which show that a twist angle of 90° is indistinguishable from an untwisted junction. [2,3] Thus, it is tempting to use this result to rule out the triplet OPs. However, as noted above, the near degeneracy of the p_{d1} -wave and p_{d2} -wave OPs in BSCCO could allow the dominant OP to twist, giving rise to a very small, but nearly isotropic $I_c(\phi_0)$. Thus, we cannot rule out the triplet states without some additional information. As mentioned above, however, such triplet states are expected to be nodeless for most of the regime $T < T_c$.

Now, the more interesting cases are the singlet spin states. There are two possibilities, states with group theoretic notation A_1 and A_2 . In Figs. 7a, 7b, and 7c, we have pictured some examples of the various possibilities. In the A_2 case, there is no s -wave compatible component, so there are quite generally twist angles ϕ_0^* at which the critical current vanishes. For the pure d_{xy} -wave OP for YBCO, or a pure $d_{x^2-y^2}$ -wave OP for BSCCO, $I_c(\phi_0^* = \pm 45^\circ) = 0$, as illustrated in Fig. 6. Similarly, for the OP case with GT notation A_2 , of a pure $g_{xy(x^2-y^2)}$ -wave OP, $I_c(\phi_0^*) = 0$ at $\phi_0^* = \pm 22.5^\circ, \pm 67.5^\circ$, as shown in Fig. 6. More generally, we then expect that there will be twist angles between these two limiting cases at which the c -axis critical current will vanish, as illustrated in Figs. 7a, 7b, and 7c. For example, if only \tilde{b}_1 and \tilde{b}_2 are non-vanishing, then the critical current vanishes at

$$\phi_0^* = \frac{1}{2} \cos^{-1} \left(\frac{-1 + [1 + 8z^2]^{1/2}}{4z} \right), \quad (15)$$

where $z = (\tilde{\eta}_4/\tilde{\eta}_2)(\tilde{b}_2/\tilde{b}_1)^2$. This expression would be modified somewhat by including $\ell = 6$ and higher order components, but the results would still show a strong anisotropy of the critical current, with some angles ϕ_0^* at which $I_c(\phi_0^*) = 0$. Of course, if the intertwist tunneling were only incoherent, but contained a small amount of d -wave incoherent tunneling ($\tau_{\perp 2} < \infty$), but no higher- ℓ -wave incoherent tunneling, then $\phi_0^* = \pm 45^\circ$.

As indicated in Fig. 7a, the A_1 state, which contains the s -wave component, can give the least anisotropic (and non-vanishing) $I_c(\phi_0)$ behavior. However, if the s -wave component is very small (Fig. 7b) or vanishes (Fig. 7c), then a highly anisotropic $I_c(\phi_0)$ can occur. In YBCO, most workers apparently believe that the OP is $|s + d_{x^2-y^2}\rangle$, which contains $d_{x^2-y^2}$ -wave and s -wave OP components. Although the experiment has not yet been performed in YBCO, this simple analysis could give a measure of the relative mixing of s -wave and $d_{x^2-y^2}$ -wave OP components in YBCO, as a function of T .

In addition, this experiment would allow for a measurement of the relative weight of coherent to incoherent tunneling, both of which are thought to be present in

overdoped YBCO, at least. Since coherent tunneling is expected to occur only for $\phi_0 = 0, \pi/2$, measuring $I_c(\phi_0)$ for ϕ_0 near to these values could give valuable information in this regard. For ϕ_0 values away from $0, \pi/2$, one could measure the relative importance of the s -wave and d -wave parts of the incoherent tunneling, along with the relative weight of each OP component as a function of T . In particular, this would give a measure of the lower limit of the amplitude of the s -wave component of the OP. To date, no such lower limit has been placed in the vicinity of T_c for YBCO.

In BSCCO, the situation is fundamentally different, as the $d_{x^2-y^2}$ -wave OP is the leading component of the A_2 state rather than the A_1 state. Thus, if the present experiments of Li *et al.* stand the test of time, the lack of any ϕ_0 dependence of I_c across the BSCCO c -axis twist junctions is *prima facie* evidence that the dominant OP is $|s + d_{xy}\rangle$, which does *not* contain any component of the purported $d_{x^2-y^2}$ -wave symmetry. Furthermore, it would be strong evidence that a $d_{x^2-y^2}$ -wave OP component (as a part of the incompatible $|d_{x^2-y^2} + g_{xy(x^2-y^2)}\rangle$ OP) could *only* appear below a second phase transition. Especially if one were to imagine that the purported $d_{x^2-y^2}$ -wave OP component were to be larger than the s -wave component, then one would require a second specific heat peak *at least* as large as that observed at T_c . In addition, the incompatibility of the s -wave and $d_{x^2-y^2}$ -wave OP components would mean that the OP containing a purported $d_{x^2-y^2}$ -wave component would be of the “ $\Delta_1 + i\Delta_2$ ” type, which would *not* have any nodes below the second transition.

We remark that the apparent absence of any ϕ_0 dependence of I_c in the vicinity of T_c does not necessarily mean that the OP is pure s -wave. It only proves that the OP is $|s + d_{xy}\rangle$ (Table V). If the intertwist tunneling were pure s -wave incoherent tunneling, one could get a ϕ_0 -independent I_c for any $|s + d_{xy}\rangle$ basis set combination, as long as the s -wave, $\ell = 0$ OP component is finite. That is, the d_{xy} -wave or $g_{x^2y^2}$ -wave OP component could even be much larger than the s -wave OP component, giving rise to nodes in the OP, and one could still observe a ϕ_0 -independent I_c . However, symmetry still requires that a ϕ_0 -independent $I_c(\phi_0)$ *precludes* the simultaneous presence of any $d_{x^2-y^2}$ -wave OP component. An example of an OP that would be roughly consistent with the \mathbf{k} -dependence of the quasiparticle gap observed in ARPES experiments (and also consistent with the c -axis twist experiments of Li *et al.*) would be the so-called “extended s -wave” OP, proportional to $|\cos(2\phi_{\mathbf{k}})|$, which is a specific example of $|s\rangle$ listed in Table II. This OP has nodes, but no $d_{x^2-y^2}$ -wave component.

We remark that it is really possible to do these experiments as a function of T , measuring $I_c(T, \phi_0)$. [3] Since the lack of ϕ_0 dependence observed just below T_c persists to low T values in all samples for which it can be measured both in the single crystal and across the twist junction,

then it most likely that the OP is *entirely* $|s + d_{xy}\rangle$, without any $d_{x^2-y^2}$ -wave component at any measurable temperature. Such a scenario would be consistent with the Pb/BSCCO c -axis Josephson tunneling results. [4] Although those authors observed very small $I_c R_n$ values, which could by themselves be interpreted as evidence for a very small s -wave component to the OP, other possible, more mundane explanations of such small values are easy to imagine, even if the superconducting OP were essentially pure s -wave. [44] For example, the same low $I_c R_n$ values were observed in NCCO, [6] which suggests that problems of a materials nature, such as an impedance mismatch in c -axis tunneling between cuprates and Pb, might be responsible for reducing $I_c R_n$.

VI. IMPROVED TRICRYSTAL EXPERIMENT PROPOSAL

We note that the tricrystal experiments of Kirtley, Tsuei, and collaborators have not been confirmed in a second laboratory. This could be due to the fact that it is very expensive to prepare the SrTiO₃ tricrystal substrates upon which the cuprate films were grown. Such depositions led to many complications at the grain boundaries, as have been evidenced by detailed transmission electron microscopy (TEM) in the case of YBCO junctions. [45] However, in the cases of other cuprates there have not been any TEM measurements available to the general public. Presumably, this is due to the large substrate costs involved.

We thus propose a new procedure, which does *not* employ any expensive tricrystal substrate, but only requires an inexpensive insulator to support the tricrystal. The improved geometry for the “tricrystal” experiment is actually constructed out of a tetracrystal ring, as pictured in Fig. 8. In this setup, a single crystal of BSCCO is cleaved twice, giving three pieces, which we illustrated as dark, intermediate, and light. The intermediate piece is cut normal to the layers into two pieces of identical thickness. The dark crystal is placed upon the support. A section of support substrate of thickness equal to that of the dark crystal is placed aside it as a support for the rest of the ring. Then, the two pieces of the intermediate crystal are placed across the dark crystal and the support, forming angles ϕ_{12} and ϕ_{23} , as pictured. The two pieces of the intermediate crystal do not touch each other. Instead, the connection between them is made by placing the light crystal on top of both intermediate crystals, forming a straight (0° or 180°) angle with one of them. Then, the entire triangular ring is fused together just below the melting point, and mounted on the insulating support. The experiment to test for the flux trapped within the tricrystal can now be performed, whether by measuring the flux within the tetracrystal with a SQUID microscope, or by applying leads, and

measuring the tetracrystal SQUID characteristics. In scanning with a SQUID microscope, one likely needs to fill the central region of the tetracrystal with an insulating material such as epoxy, and to make the triangular central region small enough to enhance the microscope sensitivity.

Let us label the crystals (1), (2), (3), and (4), clockwise beginning with the intermediately-shaded crystal in the lower right-hand part of Fig. 8. Then, the angles of the junctions as one goes around the tetracrystal are ϕ_{12} , ϕ_{23} , $\phi_{34} = 0^\circ$ or 180° , and $\phi_{41} = \pm\phi_{31}$. For each of the four junctions in this tetracrystal, the critical current can be calculated for the OP eigenfunction appropriate for the BSCCO crystal symmetry, taking into account the Josephson coupling strengths. If the s -wave OP component dominates, as in the experiment of Li *et al.*, I_c would be predicted to have the same sign across each of the junctions, so that the number of π -junctions would be 0. However, if the $d_{x^2-y^2}$ OP component dominates, then the critical currents behave as $I_{c12} \cos(2\phi_{12})$, $I_{c23} \cos(2\phi_{23})$, $\pm I_{c34}$, and $\pm I_{c41} \cos[2(\phi_{12} + \phi_{23})]$, where the \pm are consistent, and relate to whether it is a 0° or 180° junction. For choices of the angles such that $\cos(2\phi_{12})$, $\cos(2\phi_{23})$ and $\cos[2(\phi_{12} + \phi_{23})]$ are all ≤ 0 , then it is easy to show for the 16 possible configurations that one is always has an odd number of π -junctions. Thus, if the $d_{x^2-y^2}$ -wave OP component dominated the c -axis Josephson tunneling, as required for a bulk d -wave superconductor, then one ought to have a half-integral flux quantum trapped in this ring at low temperatures. More complicated scenarios such as those pictured in Figs. 7a, 7b, and 7c can be investigated by varying the tricrystal junction angles. Note that for each case in these figures for which $I_c(\phi_0^*) = 0$, the relevant I_c changes sign at ϕ_0^* . When only one junction is studied, the choice of phase factor across the junction is arbitrary, and that which minimizes the free energy of the junction changes I_c to $|I_c|$ when $I_c < 0$. But, for a tricrystal (or tetracrystal), the relative phases across the junctions are fixed, due to the loop.

The free energy of a ring with n Josephson junctions is given by

$$F = LI^2/2 - (\Phi_0/2\pi) \sum_{i=1}^n I_{ci,i+1} \cos(\Delta\varphi_{i,i+1}), \quad (16)$$

where

$$\sum_{i=1}^n \Delta\varphi_{i,i+1} = -2\pi\Phi/\Phi_0$$

$$LI^2/2 = (\Phi - \Phi_{\text{ext}})^2/2L. \quad (17)$$

These were only written down for Josephson junctions in the ab -plane, as in the tricrystal experiments of Kirtley and Tsuei. [8,32,47] However, they also apply to the case

of a ring of c -axis Josephson junctions. One has only to be careful that the self-inductance L is sufficiently large that $\beta = LI_c/\Phi_0 \gg 1$, where I_c is the minimum value of the critical currents across the junctions. [46] For the ab -plane junctions, although J_c is large, the junction area is small enough that $I_c \approx 2$ mA might not be large enough relative to L . [8] Although J_c for the c -axis junctions is much smaller than for the ab -junctions, the much larger junction areas make $I_c \approx 20 - 200$ mA, typically larger than for the ab -plane junctions. [3] Since L is proportional to the area inside the ring, by making the ring out of large single crystals, it should be possible to construct rings with $\beta \gg 1$. However, in order not to lose the SQUID sensitivity, the central area inside the ring should be nearly as small as for the ab -plane tricrystal experiments, with a rather flat insulating support for the SQUID microscope.

We remark that in the previous (ab -plane) tricrystal experiments, the dependence of the critical current I_c^{ij} upon the misalignment angles θ_i and θ_j was assumed to be proportional to either $\cos(2\theta_i)\cos(2\theta_j)$ or $\cos[2(\theta_i + \theta_j)]$, for coherent or incoherent ab -plane tunneling, respectively. However, all published experiments on YBCO showed an *exponential* dependence upon the misalignment angle $\theta = \theta_i + \theta_j$. [48–51] In the range of misalignment angles used in those ab -plane tricrystal experiments, both of the above theoretical predictions are inaccurate by several orders of magnitude. [8]

Gurevich and Pashitskii showed recently that the exponential dependence on misalignment angle observed experimentally in such YBCO ab -plane junctions is completely unrelated to any purported OP symmetry, as they were able to fit the data equally well with s -wave and $d_{x^2-y^2}$ -wave OP models, assuming the presence of insulating dislocation cores and OP suppression at the grain boundaries. [52] Such grain boundary suppression is likely to be accompanied by oxygen stoichiometry variation and hence local magnetic moments, which could be responsible for the π -junctions apparently observed in those experiments. [51] Such problems are evidently not present in the c -axis twist experiments, however. [3] Thus, our proposed new type of tricrystal (or tetracrystal) experiment is several orders of magnitude more reliable than is the ab -plane tricrystal experiment.

VII. CONCLUSIONS

We have presented tables of the allowed OP eigenfunctions for tetragonal cuprates such as Hg1201 and NCCO, and for the orthorhombic cuprates YBCO and BSCCO. For tetragonal crystals, the possible spin singlet OPs are $|s\rangle$, $|d_{x^2-y^2}\rangle$, $|d_{xy}\rangle$, and $|g_{xy(x^2-y^2)}\rangle$, the eigenfunctions of which are listed in Tables II and III. For YBCO, the spin singlet OPs are $|s + d_{x^2-y^2}\rangle$ and $|d_{xy} + g_{xy(x^2-y^2)}\rangle$, with eigenfunctions listed in Table IV. For BSCCO, the

spin singlet OPs are $|s + d_{xy}\rangle$ and $|d_{x^2-y^2} + g_{xy(x^2-y^2)}\rangle$, with eigenfunctions listed in Table V.

We distinguished between compatible OP components, which are elements of the same OP basis set, and incompatible OP components which are elements of different OP basis sets. Specifically, the s -wave and $d_{x^2-y^2}$ -wave OP components are compatible in YBCO, but incompatible in BSCCO. Compatible OP components have amplitudes which are in phase each other, and do not require the occurrence of a second phase transition to exist below T_c . Neither do any of them require a second transition to become large at low T . Incompatible OP components, on the other hand, do not mix just below T_c . Whichever has the higher bare T_c value dominates just below T_c , and the other can only become non-vanishing below a second phase transition. These incompatible OP components are then $\pi/2$ out of phase with each other below the second transition.

In addition, we evaluated the dependence of the c -axis critical current upon the twist angle ϕ_0 for each of the compatible OP eigenfunctions appropriate for each of these crystal symmetries. We have discussed these results with regard to the very recent results of Li *et al.* on c -axis twist junctions of BSCCO. [2,3] These experiments do not show any ϕ_0 dependence of the c -axis critical current density just below T_c . As a minimum, these experiments indicate that the OP is $|s + d_{xy}\rangle$.

If the intertwist tunneling were predominantly coherent, this would further imply that the OP was very nearly isotropic, having an $\ell = 0$ s -wave form, with any additional components of the $|s + d_{xy}\rangle$ OP being too small to observe. However, the more likely scenario (for BSCCO, especially) is that the intertwist tunneling is entirely incoherent, and strongly dominated by the s -wave incoherent tunneling matrix element, such that $|J|^2 = 0$ and $\tau_{\perp 0}/\tau_{\perp \ell} \ll 1$ for $\ell \neq 0$. In this case, $\tilde{\eta}_\ell \approx \delta_{\ell 0}$ in Table VII, and the c -axis twist experiments only prove that the OP contains an $\ell = 0$, s -wave component, and is thus $|s + d_{xy}\rangle$. As such, the experiments do not rule out the possibility of OP nodes. Such a scenario *could* be consistent with the quasiparticle gap observed in ARPES, [18,19] with the linear, low- T in-plane magnetic penetration depth measurements, [20] and with the Raman scattering. [22]

Assuming the OP is $|s + d_{xy}\rangle$, if the ARPES measurements were indeed giving information related to the superconducting OP, indicating nodes (or near-nodes) at $\phi_{\mathbf{k}} = \pm 45^\circ$, then the OP would have to be similar to the “extended s -wave” form, $|\cos(2\phi_{\mathbf{k}})|$. This would mean, of course, that the sign of the OP was constant. It would also mean that the amount of the d_{xy} -wave OP component relative to the magnitude of the entire OP would be small. However, if the OP did not actually change sign, then it would be difficult to explain the impurity dependence of the in-plane penetration depth. In addition, the linear, low- T dependence of the out-of-plane penetration

depth, $\lambda_c(T)$ would be difficult to explain if the intrinsic interlayer tunneling were incoherent. [20] Hence, some of these experiments might require new theoretical explanations.

For either predominantly coherent or incoherent intertwist tunneling, the c -axis twist experiments of Li *et al.* still demonstrate the *absence* of any purported $d_{x^2-y^2}$ -wave OP component near to T_c . Since s -wave and $d_{x^2-y^2}$ OP components are incompatible, any $d_{x^2-y^2}$ -wave component could *only* occur below a second phase transition. For its amplitude to be large at low T_c , the magnitude of the specific heat anomaly required at the second phase transition would have to be comparable in magnitude to the anomaly at T_c , which can be ruled out. Thus, while these experiments do not preclude a small $d_{x^2-y^2}$ -wave component at low T , they are inconsistent with a small one near to T_c , and also with a large one at low T . As such, these new phase-sensitive c -axis twist experiments are in direct conflict with the recent tricrystal experiments of Tsuei and Kirtley involving BSCCO. [17]

It remains to be seen if the same results can be obtained in YBCO, NCCO, and Hg1201. In YBCO, since the s -wave and $d_{x^2-y^2}$ -wave OP components are compatible, one can not be as clear about the possible mixing. Nevertheless, this experiment allows us to place limits upon the purported mixing of s -wave and $d_{x^2-y^2}$ -wave OP components as a function of T . In no other phase-sensitive experiment has this been yet possible in the vicinity of T_c .

Finally, we proposed that this technique can be modified to prepare a tetracrystal, which can have the desired characteristics of the tricrystal experiments of Kirtley, Tsuei, and collaborators. However, in this case, the quality of the junctions would presumably be improved by many orders of magnitude. In addition, they do not require any expensive substrates, so it should be relatively easy and inexpensive to reproduce these experiments in other laboratories.

ACKNOWLEDGMENTS

The authors thank R. C. Dynes, K. Gray, R. Kleiner, Q. Li, M. B. Maple, P. Müller, and M. R. Norman for useful discussions. This work was supported by USDOE-BES Contract No. W-31-109-ENG-38, by NATO Collaborative Research Grant No. 960102, and by the DFG through the Graduiertenkolleg “Physik nanostrukturierter Festkörper.”

- [1] Y. Zhu, Q. Li, Y. N. Tsay, M. Suenaga, G. D. Gu, and N. Koshizuka, *Phys. Rev. B* **57**, 8601 (1998); Q. Li, Y. N. Tsay, Y. Zhu, M. Suenaga, G. D. Gu, and K. Koshizuka, *Physica C* **282-287**, 1495 (1997); Y. Zhu, L. Wu, J.-Y. Wang, Q. Li, Y. N. Tsay, and M. Suenaga, *Microsc. Microanal. Microstruct.* **3**, 423 (1997).
- [2] Y. N. Tsay, Q. Li, Y. Zhu, M. Suenaga, G. D. Gu, and N. Koshizuka, in *Superconducting Superlattices II: Native and Artificial*, I. Bozovic and D. Pavuna, editors, *Proceedings of SPIE* **3480**, 21 (1998).
- [3] Q. Li, Y. N. Tsay, M. Suenaga, R. A. Klemm, G. D. Gu, and N. Koshizuka, unpublished.
- [4] R. Kleiner, M. Möhle, W. Walkenhorst, G. Hechtfisher, K. Schlenga, and P. Müller, *Physica C* **282-287**, 2435 (1997); M. Möhle and R. Kleiner, *Phys. Rev. B* (in press).
- [5] A. Bhattacharya, I. Žutić, O. T. Valls, A. M. Goldman, U. Welp, and B. Veal, unpublished.
- [6] S. I. Woods, A. S. Katz, T. L. Kirk, M. C. de Andrade, M. C. Maple, and R. C. Dynes, *IEEE Trans. Appl. Supercond.* (in press).
- [7] A. Hosseini, S. Kamal, D. A. Bonn, R. Liang, and W. N. Hardy, *Phys. Rev. Lett.* **81**, 1298 (1998); D. A. Bonn, S. Kamal, K. Zhang, R. Liang, and W. N. Hardy, *J. Phys. Chem. Solids* **56**, 1941 (1995).
- [8] C. C. Tsuei, J. R. Kirtley, C. C. Chi, L. S. Yu-Jahnes, A. Gupta, T. Shaw, J. Z. Sun, and M. B. Ketchen, *Phys. Rev. Lett.* **73**, 593 (1994); J. R. Kirtley, C. C. Tsuei, M. Rupp, J. Z. Sun, L. S. Yu-Jahnes, A. Gupta, M. B. Ketchen, K. A. Moler, and M. Bhusahn, *ibid.* **76**, 1336 (1996).
- [9] A. G. Sun, D. A. Gajewski, M. B. Maple, and R. C. Dynes, *Phys. Rev. Lett.* **72**, 2267 (1994); A. G. Sun, A. Truscott, A. S. Katz, R. C. Dynes, B. W. Veal, and C. Gu, *Phys. Rev. B* **54**, 6734 (1996); A. S. Katz, A. G. Sun, R. C. Dynes, and K. Char, *Appl. Phys. Lett.* **66**, 105 (1995); R. Kleiner, A. S. Katz, A. G. Sun, R. Summer, D. A. Gajewski, S. H. Han, S. I. Woods, E. Dantsker, B. Chen, K. Char, M. B. Maple, R. C. Dynes, and J. Clarke, *Phys. Rev. Lett.* **76**, 2161 (1996); J. Lesueur, M. Aprili, A. Goulon, T. J. Horton, and L. Dumoulin, *Phys. Rev. B* **55**, R3398 (1997).
- [10] K. A. Kousnetzov, A. G. Sun, B. Chen, A. S. Katz, S. R. Bahcall, J. Clarke, R. C. Dynes, D. A. Gajewski, S. H. Han, M. B. Maple, J. Gianpintzakis, J.-T. Kim, and D. M. Ginsberg, *Phys. Rev. Lett.* **79**, 3050 (1997).
- [11] J. Chen, J. F. Zasadzinski, K. E. Gray, J. L. Wagner, D. G. Hinks, K. K. Kousnetzov, and L. Coffey, *IEEE Trans. Appl. Supercond.* **5** (2), 1502 (1995).
- [12] L. Ozyuzer, Z. Yusuf, J. F. Zasadzinski, R. Mogilevsky, D. G. Hinks, and K. E. Gray, *Phys. Rev. B* **57**, R3245 (1998).
- [13] M. Kang, G. Blumberg, M. V. Klein, and N. N. Kolesnikov, *Phys. Rev. Lett.* **77**, 4434 (1996).
- [14] C. C. Tsuei, J. R. Kirtley, M. Rupp, J. Z. Sun, A. Gupta, M. B. Ketchen, C. A. Wang, Z. F. Ren, J. H. Wang, and M. Bhushan, *Science* **271**, 329 (1996).
- [15] J. L. Wagner, O. Chmaissem, J. D. Jorgensen, D. G. Hinks, P. G. Radaelli, B. A. Hunter, and W. R. Jensen, *Physica C* **277**, 170 (1997).
- [16] D. H. Wu, J. Mao, S. N. Mao, J. L. Peng, X. X. Xi, T. Venkatesan, R. L. Greene, and S. M. Anlage, *Phys. Rev. Lett.* **70**, 85 (1993).
- [17] J. R. Kirtley, in *Proceedings of the NATO Advanced Research Workshop on Symmetry and Pairing in Superconductors*, Yalta, Ukraine, edited by M. Ausloos and S. Kruchinin (Kluwer, Dordrecht) (in press); C. C. Tsuei, in *Proceedings of SPIE conference 3481 on Oxide Superconductors and Nanoengineering III*, San Diego, CA, edited by D. Pavuna and I. Bozovic, *SPIE* **3481** (in press).
- [18] H. Ding, T. Yokoya, J. C. Campuzano, T. Takahashi, M. Randeria, M. R. Norman, T. Mochiku, K. Kadowaki, and J. Giapintzakis, *Nature (London)* **382**, 51 (1996); H. Ding, J. C. Campuzano, A. F. Bellman, T. Yokoya, M. R. Norman, M. Randeria, T. Takahashi, H. Katayama-Yoshida, T. Mochiku, K. Kadowaki, and G. Jennings, *Phys. Rev. Lett.* **74**, 2784 (1995).
- [19] Z.-X. Shen, D. S. Dessau, B. O. Wells, D. M. King, W. E. Spicer, A. J. Arko, D. Marshall, L. W. Lombardo, A. Kapitulnik, P. Dickenson, S. Doniach, J. DiCarlo, A. G. Loeser, and C. H. Park, *Phys. Rev. Lett.* **70**, 1553 (1993).
- [20] T. Jacobs, S. Sridhar, Q. Li, G. D. Gu, and N. Koshizuka, *Phys. Rev. Lett.* **75**, 4516 (1995); S. Sridhar, private communication.
- [21] N. Miyakawa, P. Guptasarma, J. F. Zasadzinski, D. G. Hinks, and K. E. Gray, *Phys. Rev. Lett.* **80**, 157 (1998).
- [22] T. P. Devereaux, D. Einzel, B. Stadlober, R. Hackl, D. H. Leach, and J. J. Neumeier, *Phys. Rev. Lett.* **72**, 396 (1994).
- [23] H. Z. Durosoy, D. Lew, L. Lombardo, A. Kapitulnik, T. H. Geballe, and M. R. Beasley, *Physica C* **266**, 253 (1996).
- [24] R. A. Klemm, C. T. Rieck, and K. Scharnberg, *Phys. Rev. B* **58**, 1051 (1998); in *Superconducting Superlattices II: Native and Artificial*, I. Bozovic and D. Pavuna, editors, *Proceedings of SPIE* **3480**, 209 (1998); R. A. Klemm, G. Arnold, C. T. Rieck, and K. Scharnberg, *Phys. Rev. B* **58**, 14 203 (1998).
- [25] R. Kleiner and P. Müller, *Phys. Rev. B* **49**, 1327 (1994).
- [26] S. Massida, J. Yu, and A. J. Freeman, *Physica C* **152**, 251 (1988).
- [27] C. G. Olson, R. Liu, D. W. Lynch, R. S. List, A. J. Arko, B. W. Veal, Y. C. Chang, P. Z. Jiang, and A. P. Paulikas, *Phys. Rev. B* **42**, 381 (1990).
- [28] J. D. Jorgensen, *Jap. J. Appl. Phys. Suppl.* **26-3**, 2017 (1987).
- [29] M. Tinkham, *Group Theory in Quantum Mechanics* (McGraw-Hill, New York, 1964).
- [30] L. P. Falicov, *Group Theory and its Physical Applications* (University of Chicago, Chicago, 1966).
- [31] J. D. Jorgensen, D. G. Hinks, O. Chmaissem, D. N. Argyriou, J. F. Mitchell, and B. Dobrowski, in *Recent Developments in High Temperatures Superconductivity*, edited by J. Klamut, B. W. Veal, B. M. Dobrowski, P. W. Klamut, M. Kazimierski (Springer-Verlag, Berlin, 1996), pp. 1-16.
- [32] J. Annett, N. Goldenfeld, and A. J. Leggett, in D. M. Ginsberg (ed.), *Physical Properties of High Temperature Superconductors V* (World Scientific, Singapore, 1996), pp. 375-461.
- [33] J. F. Annett, N. Goldenfeld, and S. F. Renn, in D. M. Ginsberg (ed.), *Physical Properties of High Temperature Superconductors II* (World Scientific, New Jersey, 1990),

- pp. 571-685; J. F. Annett, Adv. Phys. **39**, 83-126 (1990).
- [34] X. B. Kan, J. Kulik, P. C. Chow, S. C. Moss, Y. F. Yan, J. H. Wang, and Z. X. Zhao, J. Mater. Res. **5**, 731 (1990).
- [35] X. B. Kan and S. C. Moss, Acta Cryst. B **48**, 122 (1992); X. B. Kan, Ph. D. Thesis, University of Houston, 1990 (unpublished).
- [36] V. Petricek, Y. Gao, P. Lee, and P. Coppens, Phys. Rev. B **42**, 387 (1990).
- [37] Y. Gao, P. Coppens, D. E. Cox, and A. R. Moodenbaugh, Acta Cryst. A **49**, 141 (1993).
- [38] Yimei Zhu, private communication.
- [39] G. Yang, P. Shang, I. P. Jones, J. S. Abell, and C. E. Gough, Phys. Rev. B **48**, 16 873 (1993).
- [40] G. Yang, P. Shang, I. P. Jones, J. S. Abell, and C. E. Gough, Physica C **260**, 103 (1996).
- [41] K. Machida, M. Ozaki, and T. Ohmi, J. Phys. Soc. Jpn. **65**, 3720 (1996).
- [42] V. Ambegaokar and A. Baratoff, Phys. Rev. Lett. **10**, 486 (1963); **11**, 104 (1963).
- [43] T. Dahm, J. Erdmenger, K. Scharnberg, and C. T. Rieck, Phys. Rev. B **48**, 3896 (1993).
- [44] M. Ledvij and R. A. Klemm, Phys. Rev. B **52**, 15 552 (1995).
- [45] D. J. Miller, T. A. Roberts, J. H. Kang, J. Talvacchio, D. B. Buchholz, and R. P. H. Chang, Appl. Phys. Lett. **66**, 2561 (1995); D. J. Miller, private communication.
- [46] C. D. Tesche and J. Clarke, J. Low Temp. Phys. **29**, 301 (1977).
- [47] M. Sigrist and T. M. Rice, J. Phys. Soc. Jpn. **61**, 4283 (1992).
- [48] D. Dimos, P. Chaudhari, and J. Mannhart, Phys. Rev. B **41**, 4038 (1990).
- [49] R. Gross and B. Mayer, Physica C **180**, 235 (1990).
- [50] Z. G. Ivanov, P. Å. Nilsson, D. Winkler, J. A. Alarco, T. Claeson, E. A. Stepantsov, and A. Ya. Tzalenchuk, Appl. Phys. Lett. **59**, 3030 (1991).
- [51] N. F. Henig, R. D. Redwing, I-Fei Tsu, A. Gurevich, J. E. Nordman, S. E. Babcock, and D. C. Larbalestier, Appl. Phys. Lett. **69**, 577 (1996).
- [52] A. Gurevich and E. A. Pashitskii, Phys. Rev. B **57**, 13 878 (1998).

FIG. 1. Two-dimensional representations of a single CuO_2 plane. (a) Idealized positions in a tetragonal crystal of the Cu (solid) and O (open circles) ion positions. (b) Group operations of a tetragonal crystal. (c) Group operations of YBCO. (d) Group operations of BSCCO

FIG. 2. $\ell \leq 4$ Even angular momentum OP basis functions appropriate for Hg1201, BSCCO and YBCO.

FIG. 3. Illustration of a c -axis twist junction with twist angle ϕ_0 .

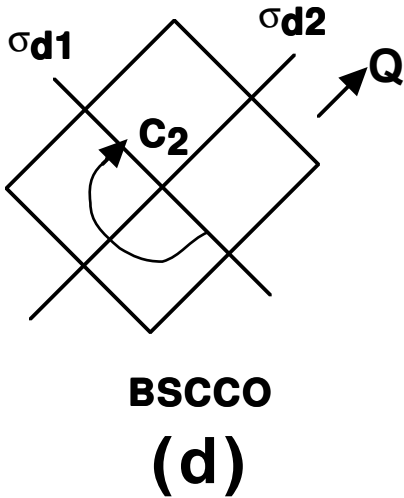
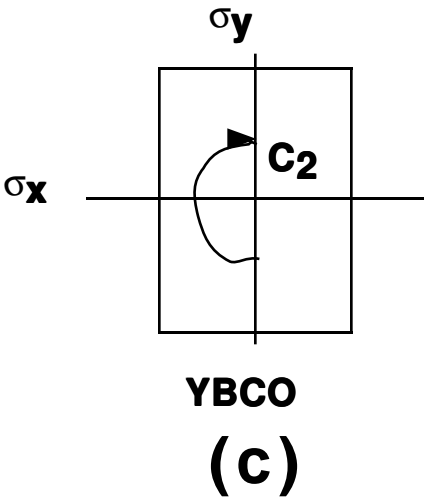
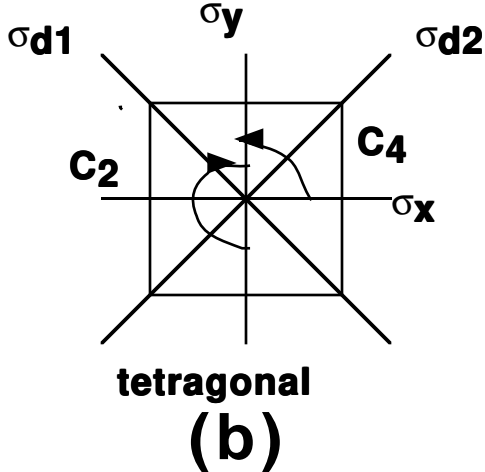
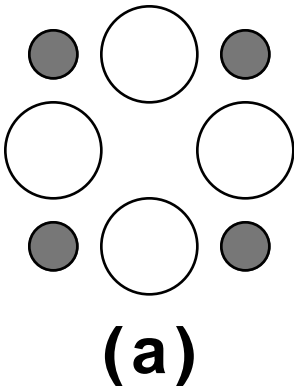
FIG. 4. (a) Tight-binding primary (thick solid curves) and secondary (thin solid and dashed) Fermi surfaces of BSCCO. The high symmetry points Γ , Y , X , and \bar{M} in the first (approximately tetragonal) Brillouin zone (BZ) are indicated, and the exact ($\Gamma - Y$) and approximate ($\Gamma - X$) mirror-plane symmetry diagonals are represented by the thin straight lines. (b) Two first BZs as in (a) rotated 45° with respect to each other.

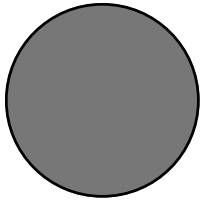
FIG. 5. Plot of $I_c(\phi_0)/I_c(0)$ for the case considered in Ref. (24) of a dominant $d_{x^2-y^2}$ -wave and subdominant d_{xy} -wave OP, the relative amounts varying with layer index away from the twist junction. The parameters for these curves are $T_{cB}/T_{cA} = 0.2$, $T_{cB}^</math>/ $T_{cA} = 0.1304$, $\epsilon/6\beta_A = 0.5$, $\delta/6\beta_A = 0.1$, and the curves for $\eta = \eta' = 0.1$ and $\eta = \eta' = 0.001$ are indicated. Curves for $t = T/T_{cA} = 0.99, 0.9, 0.5$ are presented.$

FIG. 6. Plot of $J_c^J(\phi_0)/J_c^S$ versus $2\phi_0/\pi$ for the simplest cases of pure s -wave (s), either d -wave (d), either p -wave (p), or either g -wave (g) OP contributions.

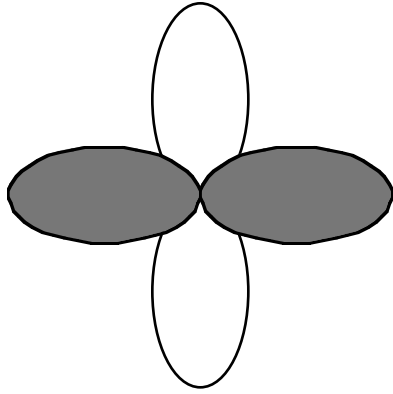
FIG. 7. Theoretical $J_c^J(\phi_0)/J_c^S$ versus $2\phi_0/\pi$ for mixed OP contributions. (a) A_1 state with $[A + B \cos(2\phi_0) + C \cos(4\phi_0)]/(A + B + C)$, and B/A , C/A ratios given. (b) Same as in (a), but with small A values. (c) A_2 state with $[B \cos(2\phi_0) + C \cos(4\phi_0)]/(B + C)$, and B/C ratios given.

FIG. 8. Proposed configuration of a c -axis version of the tricrystal ring experiment. Dark crystal: bottom. Light crystal: top. Intermediate shading: equal thickness crystals. Arrows indicate the direction of a given single crystal axis.

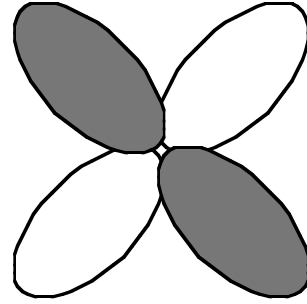




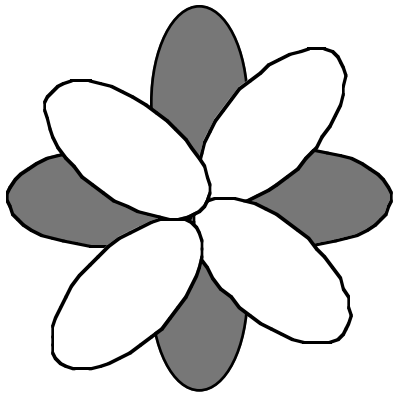
s



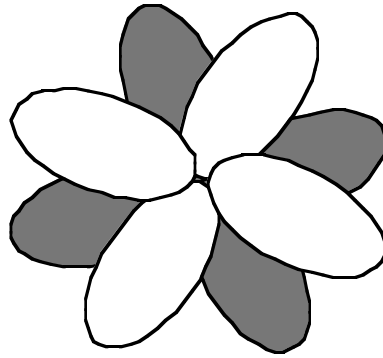
dx^2-y^2



dxy

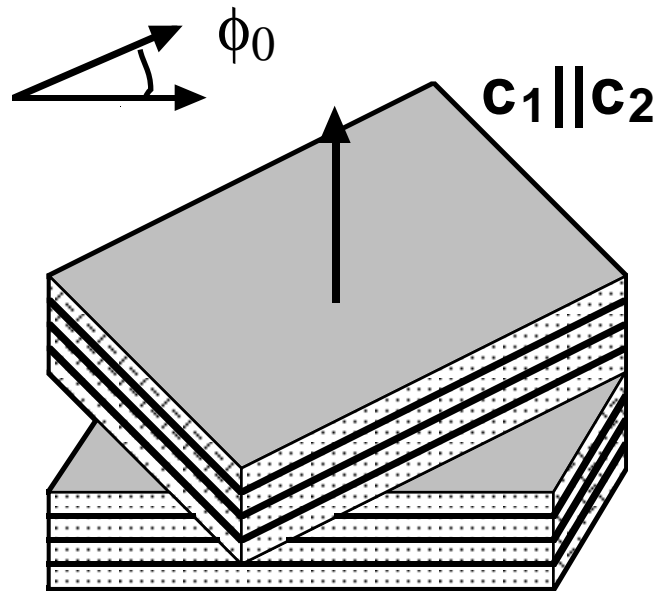


gx^2y^2



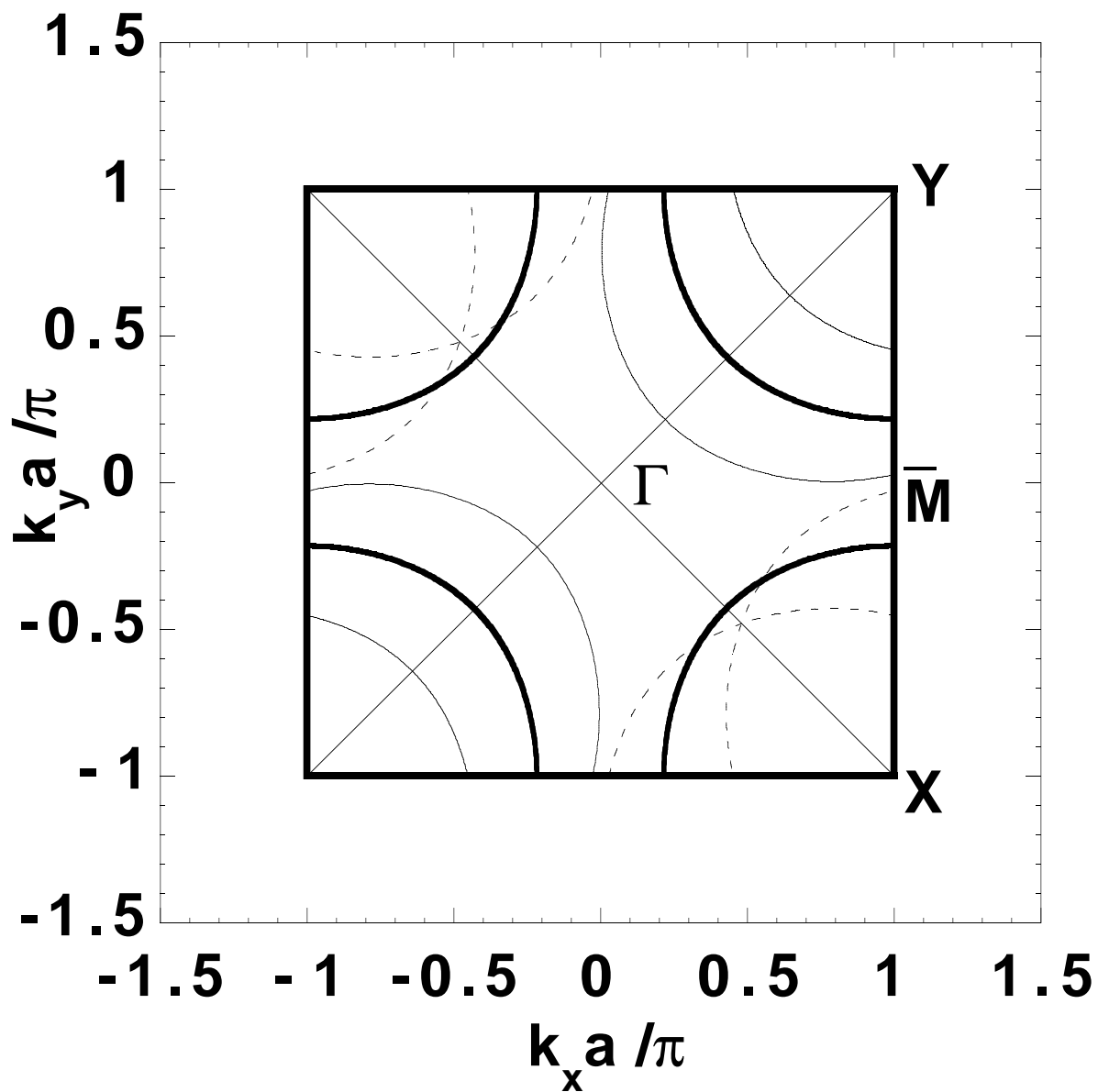
$gxy(x^2-y^2)$

Klemm Figure 2

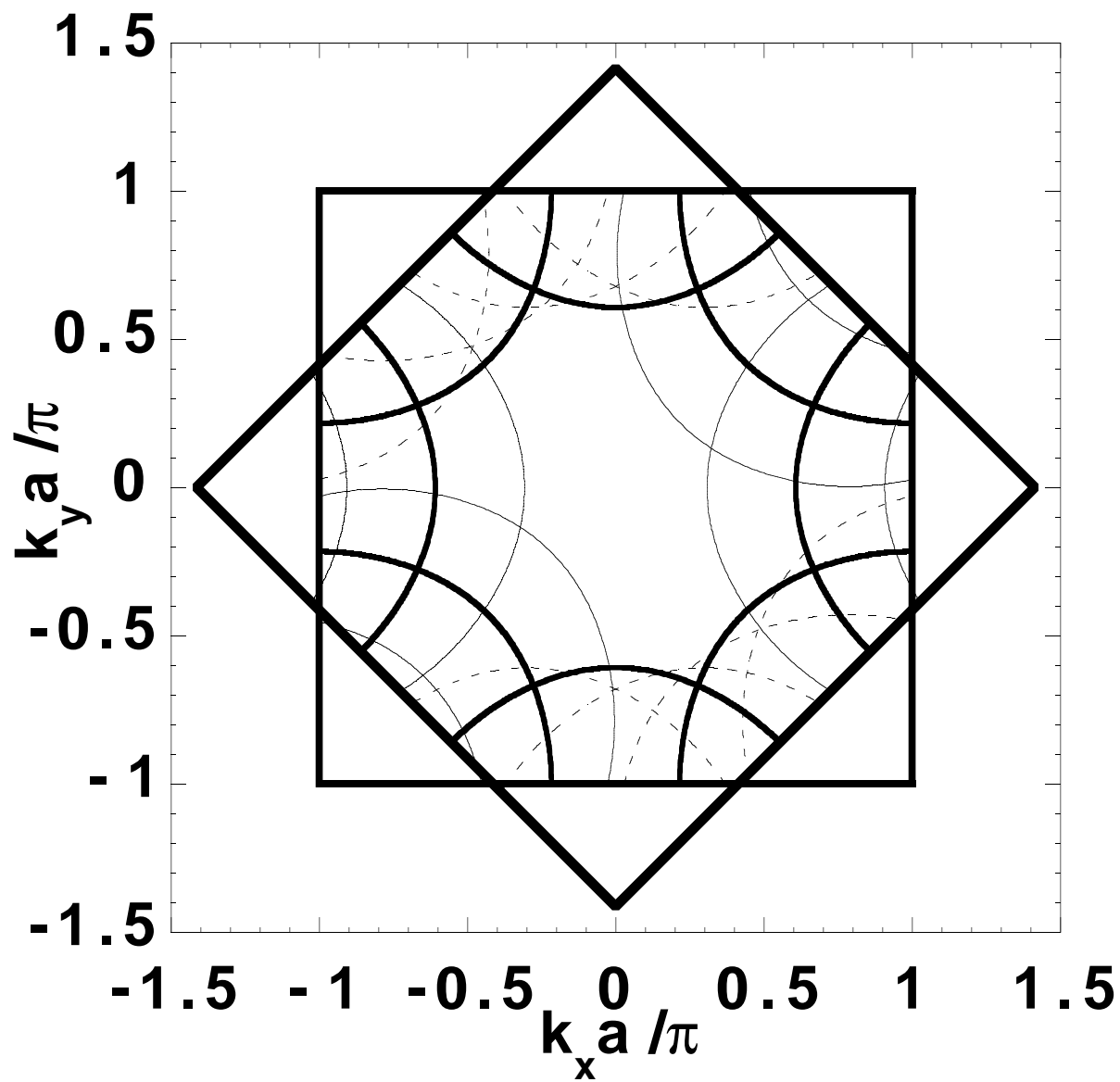


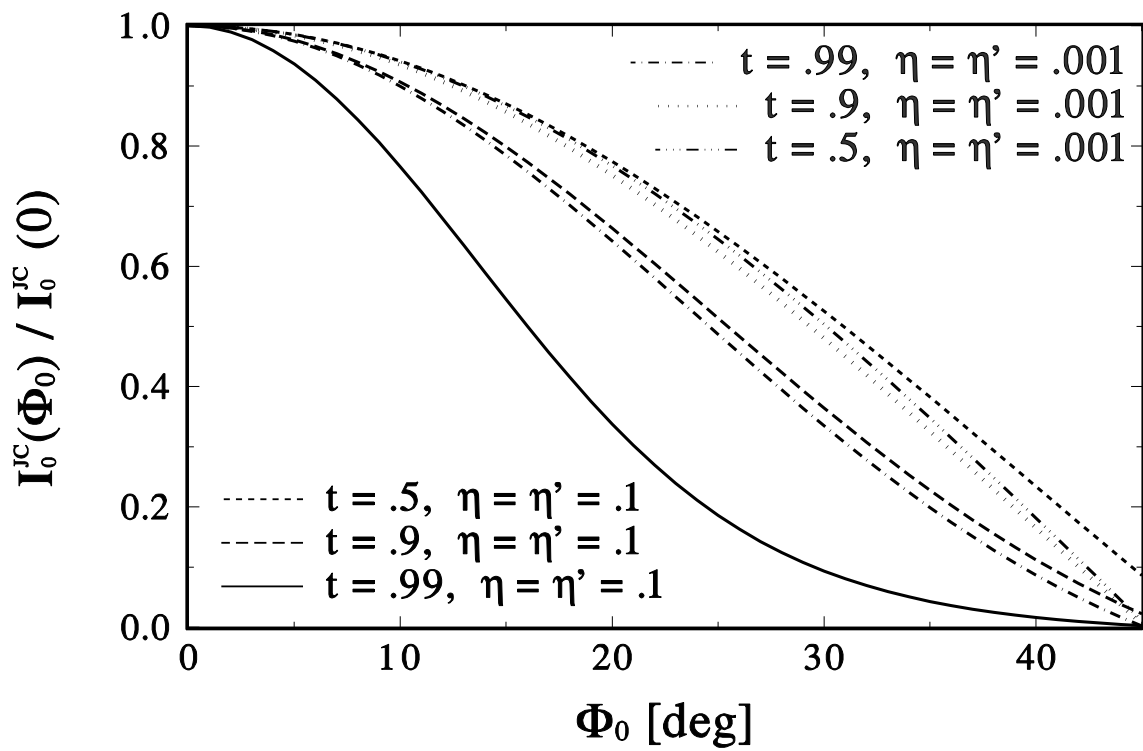
Klemm Figure 3

Klemm Figure 4a

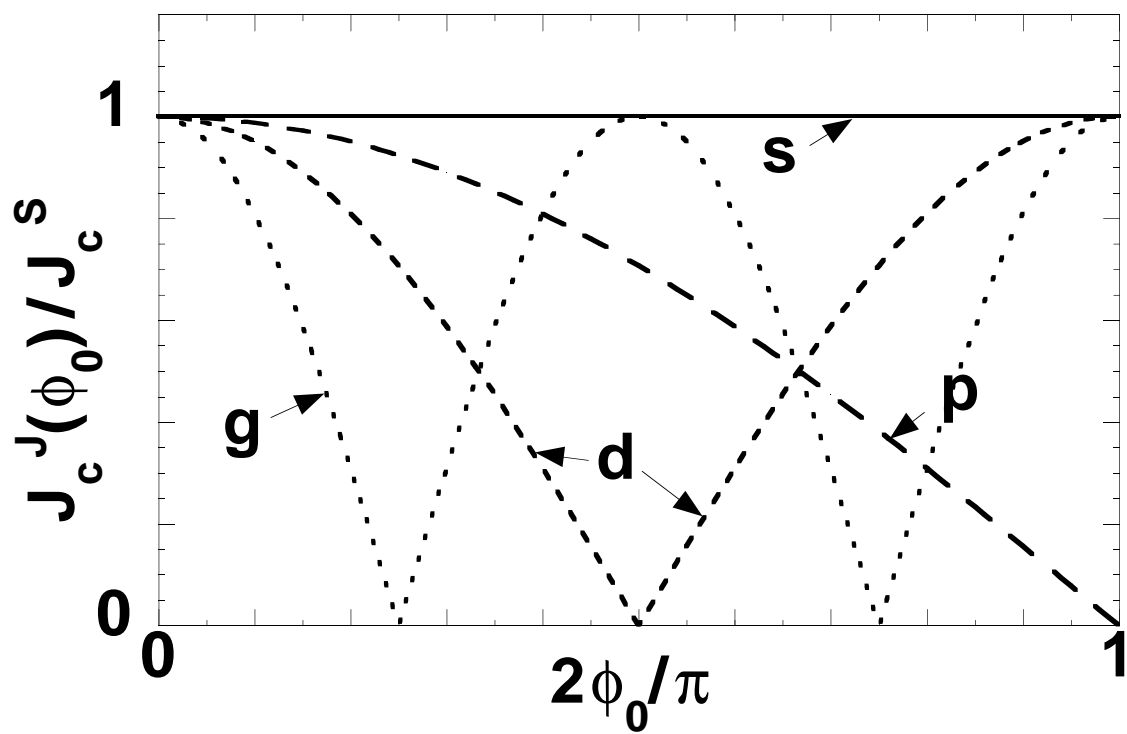


Klemm Figure 4b

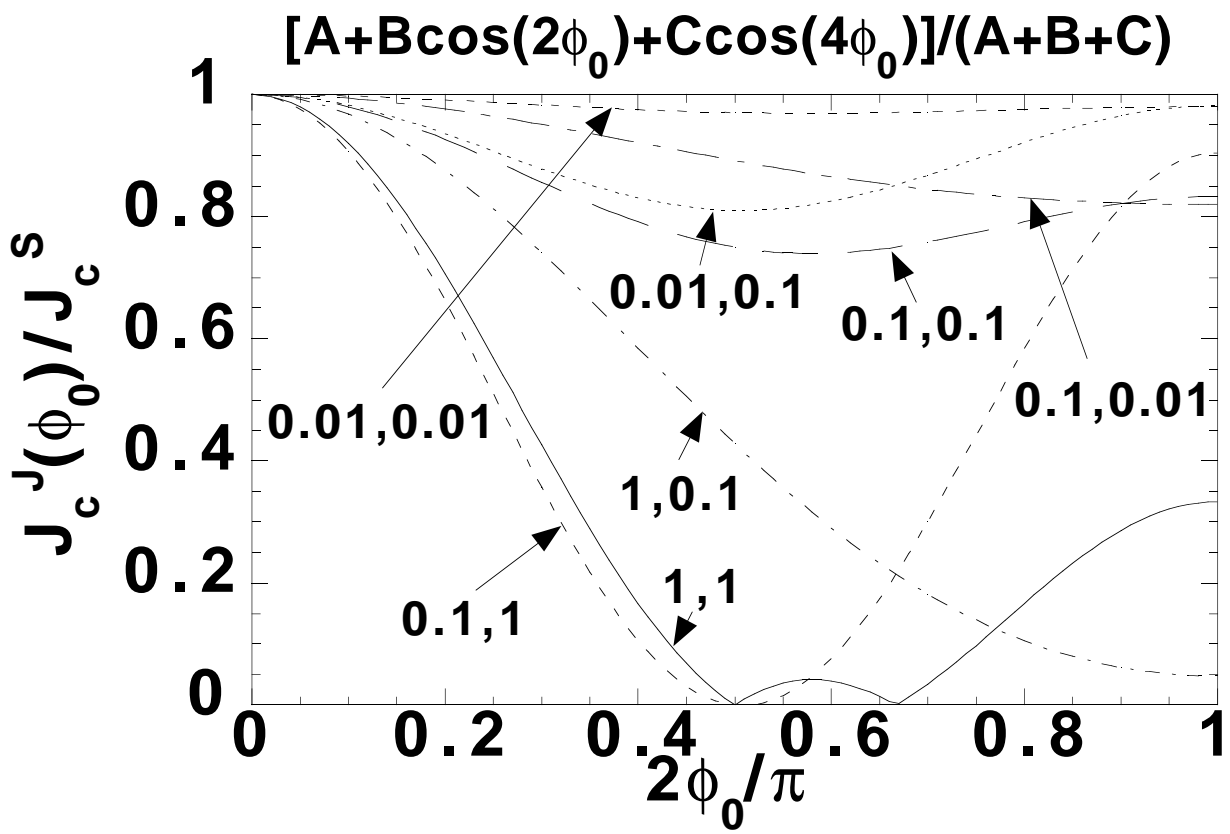




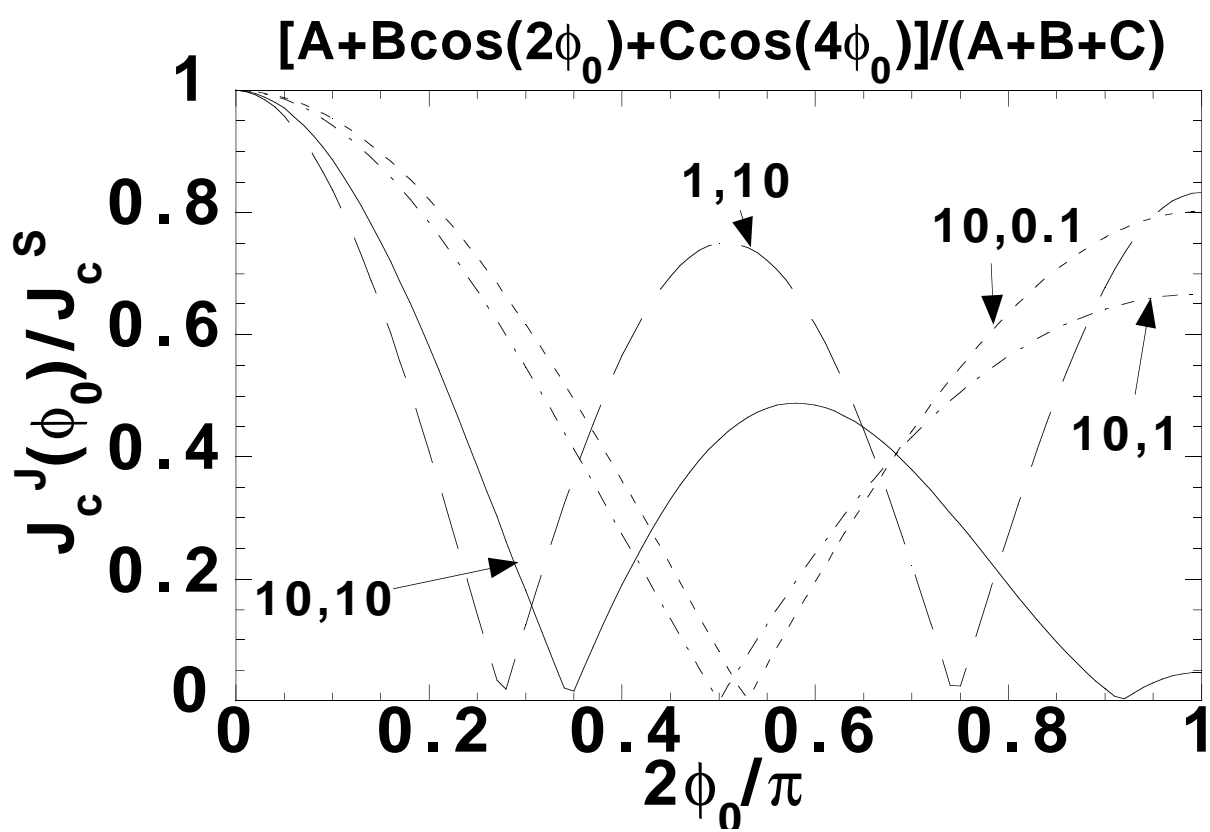
Klemm Figure 6



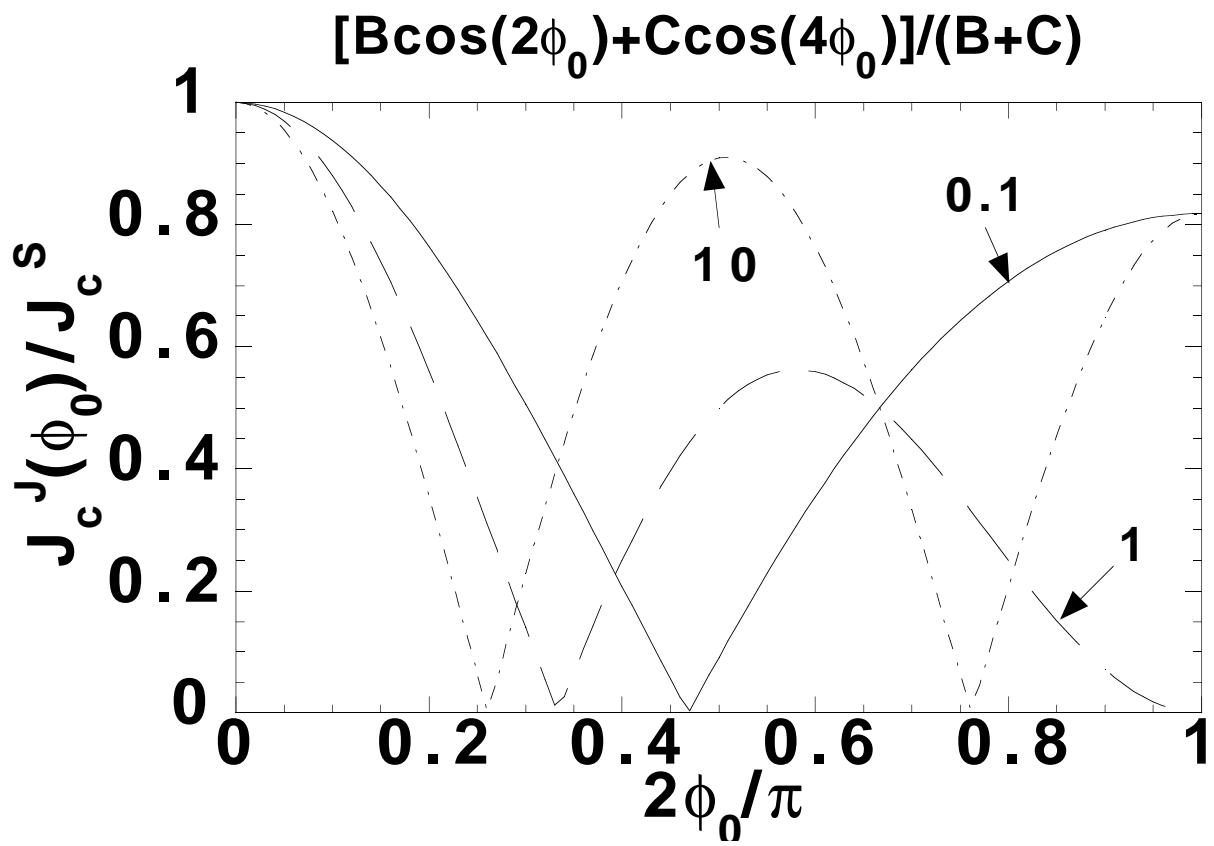
Klemm Figure 7a

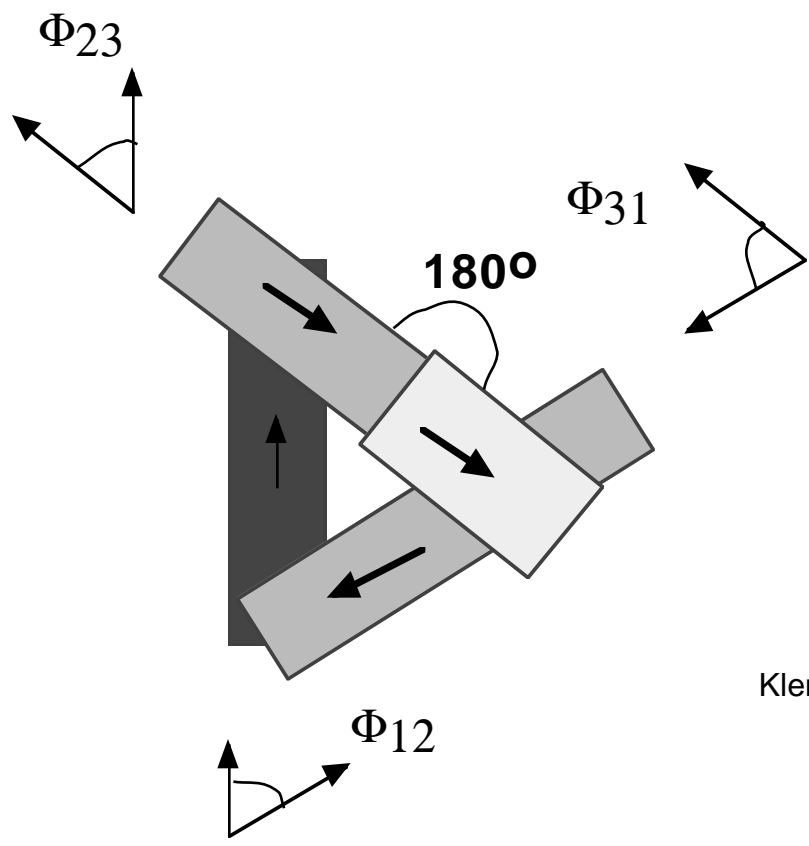


Klemm Figure 7b



Klemm Figure 7c





Klemm Figure 8